LATVIAN JOURNAL of PHYSICS and TECHNICAL SCIENCES

ISSN 0868 - 8257

5

Institue of Physical Energetics-70

(Vol. 53)

2016

LATVIAN JOURNAL of PHYSICS and TECHNICAL SCIENCES

LATVIJAS FIZIKAS un TEHNISKO ZINĀTŅU ŽURNĀLS

ЛАТВИЙСКИЙ ФИЗИКО-ТЕХНИЧЕСКИЙ ЖУРНАЛ

Published six times a year since February 1964
Iznāk sešas reizes gadā kopš 1964. gada februāra
Выходит шесть раз в год с февраля 1964 года

5 (Vol. 53) • 2016

RĪGA

Ind. pasūt. € 1,50 Indekss 2091
Org. € 15,00 Indekss 2092

SATURS

Price to individual subscribers € 1.50/issue Index 2091
Price to collective subscribers € 15.00/issue Index 2092

CONTENTS

Индивид. заказ. € 1,50 Индекс 2091
Орг. заказ. € 15,00 Индекс 2092

СОДЕРЖАНИЕ

INDEKSĒTS (PUBLICĒTS) | INDEXED (PUBLISHED) IN

www.scopus.com
www.degruyter.com
EBSCO (Academic Search Complete, www.epnet.com), INSPEC (www.iee.org.com).
VINITI (www.viniti.ru), Begell House Inc/ (EDC, www.edata-center.com).

Izdevējs: Fizikālās enerģētikas institūts
Reģistrācijas apliecība Nr. 0221
Redakcija: Aizkraukles ielā 21, Rīga, LV-1006
Tel. 67551732, 67558694
e-pasts: ezerniec@edi.lv
Interneta adrese: www.fei-web.lv
Iespiests SIA "AstroPrint"

IEGULDĪJUMS TAVĀ NĀKOTNĒ

Conference "Baltic Applied Astroinformatics and Space Data Processing"

BAASP 2015 – 4th International Scientific Conference

Astroinformatics is at the intersection of astronomy/astrophysics and applied computer science and engineering, appeared from the need to address the challenges and opportunities of exponential growth of data volumes and complexity from next-generation telescopes. Astroinformatics is the implementation of data-driven, computationally enabled science in the 21st century.

The conference "BAASP 2015" took place on 20–21 August, 2015 in the premises of Ventspils University College, Ventspils, Latvia. The previous BAASP conferences took place in Ventspils (in 2012 and 2013) and Tartu (in 2014). There were 20 presentations at the BAASP 2015 devoted to radio interferometry of space objects, design of space-related apparatus and electronic equipment (especially the artificial Earth satellites), radio astronomical observations of the Sun and their interpretation, mathematical theory of polarized radiative transfer, and remote sensing of the Earth from space. The participants of the conference were from Estonia, Latvia, Russia and Ukraine.

The three papers by F.Bushuev et al., N.Dugin et al. and M.Nechaeva et al. make up part of the proceedings of the BAASP 2015 conference. Not all the participants were willing to publish full-size papers based on their presentations. Besides, a couple of papers will be published in the next issue of "Space Research Review" issued by Ventspils University College. However, the papers hereafter give some insight into the topics discussed at the conference.

The BAASP 2015 conference was financed by the project "Development of International Collaboration and Scientific Excellence of Ventspils University College" (project No. 2015/0013/2DP/2.1.1.2.0/14/APIA/VIAA/008 financed by the European Regional Development Fund) and the project "Advanced Radio Astronomy in Europe" / RadioNet 3 (project No. 283393).

Juris Freimanis,
Chairman of the Scientific Organizing Committee of BAASP 2015

LATVIAN JOURNAL OF PHYSICS AND TECHNICAL SCIENCES
2016, N 5

DOI: 10.1515/lpts-2016-0031

RESULTS OF THE ONGOING MONITORING OF THE POSITION OF A GEOSTATIONARY TELECOMMUNICATION SATELLITE BY THE METHOD OF SPATIALLY SEPARATED BASIS RECEIVING OF DIGITAL SATELLITE TELEVISION SIGNALS

F. Bushuev[1], M. Kaliuzhnyi[1], Y. Sybiryakova[1], O. Shulga[1], S. Moskalenko[2], O. Balagura[3], V. Kulishenko[4]

[1] "Nikolaev Astronomical Observatory" Research Institute (RI NAO), 1 Observatorna Str., Mykolaiv, 54030, UKRAINE

[2] Western Centre of Radio Engineering Surveillance (WCRES), Kosmonavtov Str., Mukachevo, 89612, UKRAINE

[3] State Enterprise "Ukrkosmos", 9 Boryspilska Str., Kyiv, 02099, UKRAINE

[4] Institute of Radio Astronomy of the National Academy of Sciences of Ukraine, 4 Chervonopraporna Str., Kharkiv, 61002, UKRAINE

The results of the ongoing monitoring of the position of geostationary telecommunication satellite Eutelsat-13B (13° East) are presented in the article. The results were obtained using a radio engineering complex (RC) of four stations receiving digital satellite television and a data processing centre. The stations are located in Kyiv, Mukachevo, Kharkiv and Mykolaiv.

The equipment of each station allows synchronous recording (by the GPS) of fragments of DVB-S signal from the quadrature detector output of the satellite television receiver. Samples of the complex signal are archived and sent to the data processing center through the Internet. Here three linearly independent slant range differences (Δr) for three pairs of the stations are determined as a result of correlation processing of received signals. Every second measured values of Δr are used to calculate Cartesian coordinates (XYZ) of the satellite in the coordinate system WGS84 by multilateration method.

The time series of Δr, X, Y and Z obtained during continuous observations from March to May 2015 are presented in the article. Single-measurement errors of Δr, X, Y and Z are equal to 2.6 m, 3540 m, 705 m and 455 m, respectively. The complex is compared with known analogues. Ways of reduction of measurement errors of satellite coordinates are considered.

The radio engineering complex could be considered a prototype of a system of independent ongoing monitoring of the position of geostationary telecommunication satellites.

Keywords*: Cartesian coordinates of geostationary satellites, DVB-S, radio interferometer.*

1. INTRODUCTION

The topicality of facility development of geostationary satellite (GEOS) ongoing monitoring is caused by the constant growth of population of the Earth geostationary zone. Continuous positioning of GEOS by terrestrial means is ensured only by radio engineering facilities. Optical observations are more accurate; hence, they are commonly used for calibration of radio engineering facilities. Errors of conventional optical devices are within 0.26″–0.91″ [1].

Radar tracking system, based on single station ranging and azimuth-elevation measurement, is the most common radio-engineering facility of positioning of geostationary satellites. Accuracy of 10″ can be obtained by the system with an antenna of 10 m diameter at frequencies of 14 GHz, while accuracy of code ranging can be a few centimeters [2]. In the DARTS system (Digital Advanced Ranging with Transport-stream Signals), special ranging packets are inserted into the DVB-S (Digital Video Broadcasting-Satellite) transport stream and transmitted simultaneously with a payload [3]. The ranging accuracy of DARTS is 5 cm.

The second remote radar is often used to increase the determination accuracy of the coordinates of the controlled geostationary satellite [4]. However, to determine more accurately the satellite azimuth measured by radar a radio interferometer is applied [4], [5]. The radio interferometer has two receivers of Ku-band downlink signals. Only 250 meters separate antennas of the receivers. This distance between the antennas allows for the appliance of a common local oscillator in the receivers. To reduce the phase distortion of the signals, RF signals are fed via cooled fiber optic lines from outputs of the antennas to inputs of mixers. The phase of the signal at the output of the receivers is determined by the discrete Fourier transform. The resulting value of phase difference is used to refine the azimuth of the satellite. The accuracy of phase difference determination is about 5 % of a wavelength or 1.2 mm for a signal frequency of 13 GHz. The corresponding directional accuracy is about 1″.

Chinese VLBI network (CVN) of four stations was used in the research [6] to calibrate the tracking system for geostationary satellites belonging to the COMPASS navigation system. Minimum baseline length of the CVN equals 1100 km, and the maximum is 3250 km. Signal transmitted by the geostationary satellites at a frequency of 2.2 GHz was used as the VLBI beacon. Spectral width of the signal was approximately 2 MHz. The accuracy of delays measured by the VLBI was 3.6 ns and the accuracy of satellite coordinate determination was 10 m.

A radio engineering complex (RC) was developed at the Research Institute NAO for active geostationary telecommunication satellite positioning [7]. The basic principle of the RC is the determination of the difference of slant ranges to a satellite from a pair of receivers using the correlation analysis of the received DVB-S signals. Hence, the proposed approach is equivalent to that used in radio interferometry. The slant range difference to an observed radio source is also obtained there as a result of the correlation analysis of the received signals. The article presents the results of measurements of the coordinates of the geostationary satellite Eutelsat-13B. The results were obtained in the period from March to May 2015 using the upgraded RC.

2. RC: TECHNIQUE, HARDWARE AND SOFTWARE

The Earth-centered Earth-fixed coordinate system is used to determine Cartesian coordinates of the tracked geostationary telecommunication satellite by the multilateration (or hyperbolic) method [8], [9]. Let (x, y, z) and (x_i, y_i, z_i) denote the desired satellite coordinates and the known coordinates of the i-th station, and let $R_i = \left[(x - x_i)^2 + (y - y_i)^2 + (z - z_i)^2\right]^{\frac{1}{2}}$ be the distance between the satellite and the i-th station. The following system of nonlinear equations can be used to find the satellite coordinates:

$$R_0 + \Delta r_i - R_i = 0, \;\; i = 1,..., I - 1 \tag{1}$$

where $\Delta r_i = c \cdot \Delta \tau_i$ – the difference between slant ranges obtained for the i-th and 0-th stations;

c – the speed of light in vacuum;

$\Delta \tau_i$ – the difference between measured delays of the DVB-S signals received by the stations;

I – the number of spaced stations.

Hence, the complex should consist of four or more stations to determine three unknown satellite coordinates.

Initial values (x^0, y^0, z^0) for the satellite coordinates are required for solving the nonlinear system of equations (1) using a numerical method. They should be defined in the same coordinate system as the coordinates of the stations. The coordinates of the stations are set in the Earth-fixed WGS84 (World Geodetic System of 1984) system because the WGS84 is the reference coordinate system used by the GPS and, therefore, the coordinates can be taken directly from the measurement data of GPS receivers used for synchronization of the stations [7]. The initial values (x^0, y^0, z^0) can be computed with the following approximate geographical coordinates of the satellite relative to the WGS84 ellipsoid: $\varphi_{GSS}, \lambda_{GSS} = 0$ и $h_{GSS} = 36000$ km, where $\varphi_{GSS}, \lambda_{GSS}$ and h_{GSS} denote the longitude, latitude and height of the geostationary satellite, respectively. Formulas for conversion between geographical and Cartesian coordinates may be found in [2], [10]. The given method of estimating (x^0, y^0, z^0) allows one to solve the system of equations (1) in a few Newton's iterations.

Currently, the RC is composed of four ($I = 4$) identical stations receiving digital satellite TV (Digital Television-Satellite (DTV-S)), which are installed in the cities of Kyiv, Mukachevo, Mykolaiv and Kharkiv. The maximum distances between the stations are about 1000 km and 400 km along longitude and latitude, respectively.

Each station consists of:

1) The standard antenna-feeder system for the reception of DTV-S signals, with antennas of 0.9 m (in Kyiv, Mukachevo and Kharkiv) and 1.9 m (in Mykolaiv) in diameter;
2) DTV-S receiver (SkyStar1 or SkyStar2) performed as a PCI-card and upgraded in terms of outputting of in-phase and quadrature signals;

3) Single-frequency ThunderBolt-E GPS receiver;
4) Digital USB-oscilloscope DSO5200A with 200 MHz passband and 9-bit ADC (Analog Digital Converter);
5) Personal computer with USB and RS-232 ports, operable in Windows XP environment (1 GHz CPU clock rate; 1 Gb RAM, and 100 Gb HD capacity);
6) Internet connection at data rate of at least 80 Kbytes per second.

Detailed description of the station hardware and software is given in [7]. The hardware and software allow each station of the RC to record every second fragments of DTV-S complex signal synchronously with PPS (Pulse-Per-Second) signals incoming from the GPS receivers. A feature of USB-oscilloscopes DSO5200A employed as ADC is the dependence of the nominal sampling frequency f_n on the duration T_s of a recorded fragment:

$$f_n = \frac{N_s}{T_s}$$

where N_s = 10240 – the constant equal to the size of sample. The value of T_s depends on the selected scale of the oscilloscope. Two factors were taken into account in the research [7] to select the oscilloscope scale. First of all, Nyquist rate for recorded DVB-S signal was defined. Then the location of stations was chosen based on the obtained maximum value of T_s. Let B denote the length of the baseline connecting the stations. The stations should be located so as to satisfy the inequality: $B \le T_s \cdot c$. The restriction on the length of the baseline was significantly weakened by using the ability to change the PPS signal delay τ_{PPS} with respect to the beginning of a second. This ability is provided in the receivers ThunderBolt-E. The difference between delays of DTV-S signals received at two stations can be represented as the sum of two terms:

$$\Delta\tau = \overline{\Delta\tau} + \hat{\tau}$$

where $\overline{\Delta\tau}$ – the average difference of the delays, and $\hat{\tau}$ – the variation of the delay difference with respect to $\Delta\tau$. The average difference of the delays $\Delta\tau$ may be a few milliseconds because it depends on the length of the baseline connecting the stations and on the relative position of tracked satellite and baseline. The variation of the delay difference $\hat{\tau}$ depends on displacement of the satellite within its geostationary slot and it cannot exceed 20 μs. If there are several pairs of stations τ_{PPS} =0 can be set for one (chosen) station. For the rest of the stations τ_{PPS} can be set equal to the value of $\Delta\tau$ with respect to the chosen station. Numerical simulation may be used to estimate $\Delta\tau$. The satellite orbital parameters required for the simulation could be found at the site: www.space-track.org. The DTV-S receivers employed in the RC can receive DVB-S signal at a symbol rate of 22000 or 27000 kSym/s. The spectral width of the signals is about 30 MHz [11]. Hence, their Nyquist rate is equal to 60 MHz. The value of f_n closest to the Nyquist rate is 51.2 MHz. It corresponds to T_s = 200 μs that is substantially greater than the possible values of $\hat{\tau}$.

Every second complex samples of DTV-S signal are archived and sent through the Internet to the processing centre in Mykolaiv. Here the following is carried out for a given pair of stations [7]:

- Transforming the complex samples in real samples taking into account the structure of the DVB-S signal;
- Computing the correlation function of the real samples;
- Computing the difference of the delays of the DVB-S signals received by the stations.

The value of $\Delta\tau_i$ is estimated by the following formula:

$$\Delta\tau_i = \left(\frac{n_{xi}}{k_{sr} \cdot f_n} + \tau_{PPSi} \right) - \left(\frac{n_0}{k_{sr} \cdot f_n} + \tau_{PPS0} \right) - \Delta\tau_{hi} . \qquad (2)$$

Expression (2), unlike that used in [7], has a number of additional parameters: τ_{PPSi} and τ_{PPS0} – given initial delays of PPS signals of GPS receivers of the stations; $\Delta\tau_{hi}$ – measured value of the difference of hardware delays of the stations; k_{sr} – measured coefficient of proportionality between a valid (f_v) and nominal sampling frequencies:

$$f_v = k_{sr} \cdot f_n .$$

It is assumed that $\Delta\tau_{hi}$ depends on equipment characteristics of the stations (e.g., on the difference of the electrical lengths of cables between antennas and receivers and so forth), and k_{sr} is the constant for the given type of USB-oscilloscope. The parameters $\Delta\tau_{hi}$ and k_{sr} are determined during calibration before sending stations to their places of observation.

In (2), n_{xi} and n_0 are measured in counts of the sampling frequency. The parameter n_{xi} is equal to the offset of the maximum of the correlation function from the beginning of the sample obtained by the *i*-th station. The position of the maximum is confirmed using the Hilbert transform of the correlation function by the method proposed in [12]. Thus, in general, the value of n_{xi} is a fractional non-negative value. The value of n_0 is also a non-negative value, but always it is integer because it equals to a given offset of the middle part of the sample obtained by the zero station. The offset is set from the beginning of the sample. The size of this middle part of the sample is always smaller than N_s, and it is equal to the sample size of correlator (N_c). The parameters n_0 и N_c are set so that variations of $\hat{\tau}$ with respect to $(\tau_{PPSi} - \tau_{PPS0})$ are within the interval $\left[\frac{-n_0}{f_v}, \frac{N_s - N_c - n_0}{f_v} \right]$.

Three linearly independent values of $\Delta\tau_i$ (i=1,..,I-1) are computed using (2). Then they are used in (1) to find every second values of the Cartesian coordinates of the tracked satellite.

Additional software is used to estimate statistical characteristics of Δr and (x, y, z).

3. OBSERVATION RESULTS

Position of ongoing observations of geostationary satellite Eutelsat-13B presented in the article was obtained by the RC during the period from 11 March 2015 to 20 May 2015. Eutelsat-13B is co-located in an orbital slot of 13° East with two other satellites, Eutelsat-13C and Eutelsat-13D. The DVB-S signal at the frequency of 11541 MHz with vertical polarization and at the symbol rate of 22000 kHz is received by the RC stations during the whole observation period, including the analysed interval. The duration of sample of recorded signals of quadrature detector is set to T_s = 200 μs. It corresponds to the nominal sampling rate f_n = 51.2 MHz that is close to the Nyquist rate for the received signal. The PPS signal delays for the stations in Kyiv, Kharkiv and Mukachevo are set in such a way as to keep zero delay for the Mykolaiv station and are equal to 888 μs, 1270 μs and –215 μs, respectively.

Differences of slant ranges changing over time are shown in Fig. 1 for the three pairs of the stations: Kharkiv-Mykolaiv, Mukachevo-Mykolaiv and Kyiv-Mykolaiv. The station in Mykolaiv is the zero station for all pairs listed in Fig. 1. As a result of the correlation analysis, the delays of the signals received in Kharkiv, Mukachevo and Kyiv are computed regarding the delay of the signal received in Mykolaiv. The y-axis of the graphs represents the values of Δr, which were obtained by averaging the every second samples of Δr at the interval of 60 seconds. The x-axis represents time (UTC) from 11 March 2015 to 20 May 2015.

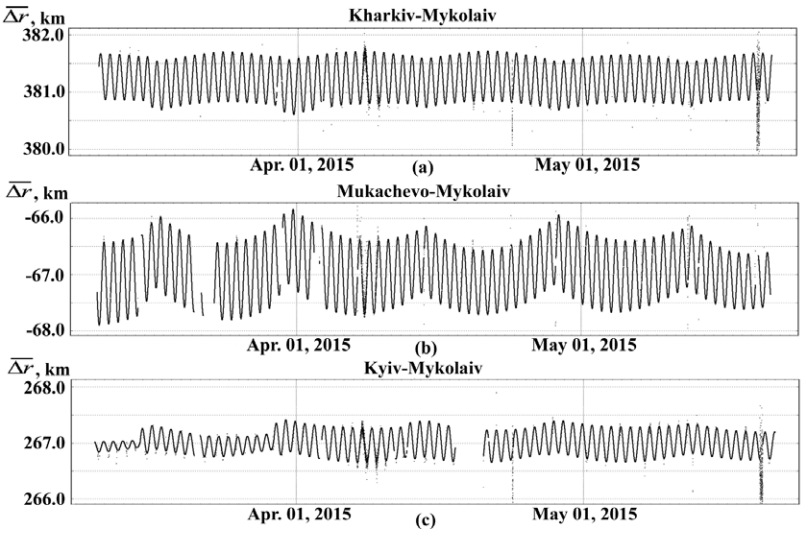

Fig. 1. Slant range differences for three pairs of stations: Kharkiv-Mykolaiv (a), Mukachevo-Mykolaiv (b) and Kyiv-Mykolaiv (c). Observation time is from 11 March 2015 to 20 May 2015.

It should be noted that there are a few specific intervals of abrupt changing in the amplitude of the diurnal variations of Δr on its graph obtained for the pair of the stations Kyiv-Mykolaiv (its baseline is oriented along latitude). Especially clearly these changes were evident in the intervals from 11 March 00:00 UTC to 15 March 16:28 UTC and from 15 March 16:28 UTC to 29 March 17:31 UTC. Obviously, the satellite orbit had been corrected on 15 March 16:28 UTC and 29 March 17:31 UTC.

Empirical probability density ($P(\sigma=\xi)$) and distribution ($P(\sigma<\xi)$) functions of values of standard deviation (SD or σ) are given in Fig. 2. The values of σ were computed at 60-second intervals of time for each of the samples presented in Fig. 1.

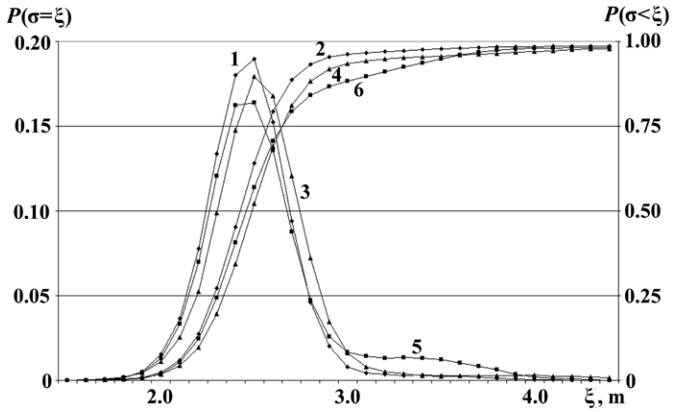

Fig. 2. Empirical probability density function (1, 3 and 5) and distribution function (2, 4 and 6) of standard deviation of slant range differences for three pairs of stations: Kharkiv-Mykolaiv (1 and 2), Mukachevo-Mykolaiv (3 and 4) and Kyiv-Mykolaiv (5 and 6). Observation time from 11 March 2015 to 20 May 2015.

From the data given in Fig. 2 it follows that the median of the SD of Δr equals 2.5 m for the pair of the stations Kharkiv-Mykolaiv and 2.6 m for the other two pairs. It should be noted that all the empirical distributions of σ given in Fig. 2 are asymmetric with respect to the median values. All three graphs $P(\sigma=\xi)$ subside more slowly in the interval (ξ >3.0) in comparison with the interval (ξ <2.2). Graph 2 obtained for the pair Kyiv-Mykolaiv has a clearly pronounced local maximum in the range of (ξ> 3.0).

Every second values of Cartesian coordinates (X, Y, Z) of Eutelsat-13B satellite are obtained in the WGS84 coordinate system by solving the system of nonlinear equations (1) for three values of DVB-S signal, relative delays measured by the RC. The corresponding graphs of averaging values of the coordinates $\overline{X}$, $\overline{Y}$, $\overline{Z}$ are given in Fig. 3. The averaging was performed in intervals of 60 seconds.

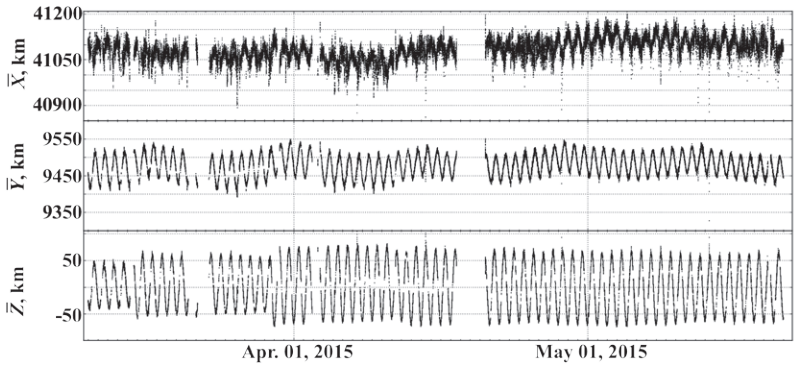

Fig. 3. Cartesian coordinates of Eutelsat-13B satellite in the WGS84. Observation time from 11 March 2015 to 20 May 2015.

It should be noted that an abrupt change in the amplitude of diurnal variations of $\overline{Z}$ is clearly visible on its graph on 15 March 16:28 UTC and 29 March 17:31 UTC, as well as on the graph of Δr obtained for the pair of the stations Kyiv-Mykolaiv (Fig. 1). These changes may be associated with the satellite orbit corrections.

Spatial positions of the tracked satellite are shown in Fig. 4. It was built according to the data shown in Fig. 3.

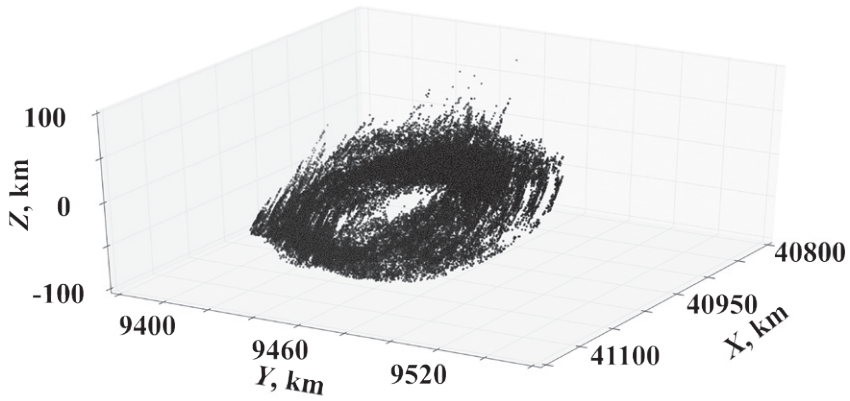

Fig. 4. Spatial positions of Eutelsat-13B satellite in the period of time from 11 March 2015 to 20 May 2015.

The following procedure of discarding of gross errors is used for constructing the graphs shown in Figs. 3 and 4. If corresponding values of Δr are discarded for at least one of the pairs of stations, averaged values of $\overline{X}$, $\overline{Y}$ and $\overline{Z}$ are discarded. If the sample size of averaging is less than 10 or the value of the SD of Δr exceeds 3.0 m, value of Δr is discarded.

Empirical probability density and distribution functions of values of standard deviations of *X*, *Y* and *Z* (σ_X, σ_Y and σ_Z, respectively) are given in Fig. 5. The values of σ_X, σ_Y and σ_Z were computed at 60-second intervals of time for all samples without discarding gross errors.

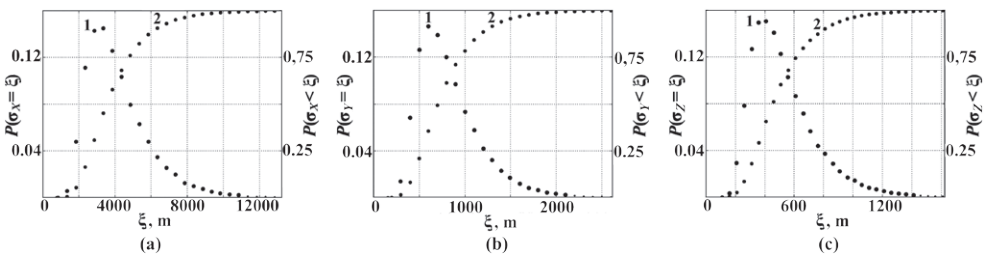

Fig. 5. Empirical probability density function (1) and distribution function (2) of standard deviation of Cartesian coordinates of Eutelsat-13B satellite in the WGS84: X – (a), Y – (b) and Z – (c).

Due to the data given in Fig. 5, the medians of standard deviations of *X*, *Y* and *Z* are equal to 3540 m, 705 m and 455 m, respectively. Hence, the coordinate *X* has larger error than *Y* and *Z*.

4. DISCUSSION

The obtained error (the standard deviation of single measurement) of slant range differences of about 2.6 m is completely determined by PPS signal accuracy of the ThunderBolt-E GPS receiver [13] and is close to the minimum error for the RC equipment composition. The minimum error is 7 ns or 2.1 m. It was obtained in the research [7]. This value is free of the RC synchronization error by the GPS and is mainly caused by the instability of oscillator frequency of the USB-oscilloscopes ADC. Thus, further reduction of the error of Δr is possible by increasing the timing accuracy, i.e., the frequency stability of the ADC reference oscillators. For example, the ThunderBolt-E GPS receivers could be replaced with GPS-disciplined rubidium frequency standards [14]. The PPS signal from the rubidium is aligned to UTC and has less than 0.3 ns jitter. An atomic rubidium oscillator of the GPS10RBN could also be used as the main frequency reference for the ADC. It should be noted that maximum error of slant range difference measurement is caused by the spectral width of the received signal. This error for DVB-S signal with a spectral width of 30 MHz is less than 1 ns or 0.3 m. The error was obtained in process [3].

Let ε_a denote the error of an angular coordinate of tracked satellite, and let B be the length of the radio interferometer baseline. In [4], the value of ε_a was equal to about 1″ and it was obtained from the following approximate ratio:

$$\varepsilon_a = \sigma / B , \tag{3}$$

for the radio interferometer with σ = 1.2 mm and B = 250 m. Relation (3) holds at small ratio of B to the distance to the satellite. Let us estimate ε_a for the RC. In this case, the value of ε_a can also be estimated from (3) because the ratio of the minimum distance between the RC stations to the distance to the satellite is significantly less than one (around 10^{-2}). Substituting σ = 2.6 m and B=400 km in (3), one finds that ε_a is also approximately equal to 1″. Thus, the RC value of ε_a coincides with the estimation obtained in [4] due to large length of the RC baseline. Thus, working together with radar, the complex would ensure the same positioning accuracy of the satellite like the radio interferometer considered in [4], [5].

The example above shows that small error value of Δr does not guarantee small value of error when determining the coordinates of satellite. It is also necessary that the stations of radio interferometer have been optimally placed in space and at enough large distance from each other. Generally, the error of coordinate determination is nonlinear function of σ and B given by the system of equations (1). The nonlinear dependence on σ and B of the coordinate errors is confirmed by comparing the accuracy of the Chinese VLBI Network [6] and two versions of the RC. The previous version of the RC (Version 0) differs from the current one (Version 1) in that the Mykolaiv station was synchronized by Resolution-T, which was less accurate than the Thunderbolt-E GPS receiver. Parameters of the radio interferometers (RI) are given in the following table where:

B_{RI} is the minimum length of baselines of the RI;

$b = \dfrac{B_{CVN}}{B_R}$ is a ratio of values of B_{RI} for the CVN and RI;

$\sigma_{\Delta r}$ and σ_{XYZ} are maximum errors for determining of Δr and Cartesian coordinates of satellite;

$s = \dfrac{(\sigma_{\Delta r})_R}{(\sigma_{\Delta r})_{CVN}}$ is a ratio of values of $\sigma_{\Delta r}$ obtained by RI and the CVN;

$v = \dfrac{(\sigma_{XYZ})_R}{(\sigma_{XYZ})_{CVN}}$ is a ratio of values of σ_{XYZ} obtained by RI and the CVN.

Table 1

Comparison of the Accuracy of the CVN and the RC

RI	B_{RI}, km / b	$\sigma_{\Delta r}$, m / s	σ_{XYZ}, m / v
CVN	1100 / 1	1 / 1	10 / 1
RC (Version 0)	400 / 2.75	4.5 / 4.5	40000 / 4000
RC (Version 1)	400 / 2.75	2.6 / 2.6	3540 / 354
RC (Version 2)	1000 / 1.1	2.6 / 2.6	≈400 / ≈40
RC (Version 3)	1000 / 1.1	0.3 / 0.3	<10 / <1

The data presented in Table 1 show that the error of slant range difference decreased by 1.7 times after the Resolution-T at the station in Mykolaiv was replaced with a more accurate GPS receiver. At the same time, the error of coordinate determination decreased by more than 10 times. The data also show that the error of coordinate determination by the current version of the RC was two orders of magnitude greater than that for the CVN, while its $\sigma_{\Delta r}$ was 2.6 times greater and its B_{RI} was less than 2.75 times. It can be concluded that relatively small changes of $\sigma_{\Delta r}$ or B_{RI} (e.g., doubled) result in significantly greater changes (10 times) of the error of coordinate determination. Taking this into account, the accuracies of two possible versions of the RC (2 and 3) are given in the last two rows of the table. The version 2 differs from the current version of the RC in that the length of the baseline along latitude is increased by more than twice to 1000 km. It can be expected that the error of coordinate determination will be decreased by about an order of magnitude, up to 400 m. The version 3 differs from the version 2 in that its error of Δr estimation is equal to the minimum possible error of 0.3 m. In this case, the error of coordinate determination can be decreased to a value of less than 10 m.

4. CONCLUSION

1. The continuous observations of the geostationary telecommunication satellite Eutelsat-13B were performed by the radio engineering complex during more than two months from 11 March 2015 to 20 May 2015. The RC consists of four stations receiving DVB-S signals and spaced at about 1000 km and 400 km along longitude and latitude, respectively.

2. According to these observations, the errors of single measurements of slant range differences and Cartesian coordinates of the tracked satellite were determined. These errors were equal to 2.6 m, 3540 m, 705 m and 455 m for Δr, X, Y and Z, respectively.

3. The estimations of errors of coordinate determination for possible modifications of the RC were obtained by comparing the accuracy characteristics of two versions of the RC and the CVN. In the case of increasing the minimum baseline of the RC to the order of 1000 km, the error of coordinate determination can be about 400 m. The estimation of the minimum possible error of geostationary satellite coordinates was also obtained. The error becomes no more than 10 m in the case of saving the minimum length of the RC baseline equal to about 1000 km, and if slant range difference is estimated with an error equal to or less than 0.3 m.

4. The complex considered can be a prototype of the system of ongoing monitoring of orbits of active geostationary telecommunication satellites. This system can be cheap to implement, fully independent and untied to uplink stations.

REFERENCES

1. Kara, I.V., Kozyryev, Y.S., Sybiryakova, Y.S., and Shulga, O.V. (2011). NAO catalog of geocentric state vectors of geosynchronous space objects. *Bulletin of the Crimean Astrophysical Observatory*, *107 (1)*, 98–102.
2. Montenbruck, O., and Gill, E. (2005). *Satellite orbits: Models, methods, and applications.* Berlin: Springer.
3. A novel ranging method using DVB-S transport stream packets [online]. Available at http://esamultimedia.esa.int/conferences/01C14/papers/P2.2.pdf.
4. Keeping track of geostationary satellite – A novel and less costly approach [online]. Available at http://www.esa.int/esapub/bulletin/bulletin119/bul119_chap8.pdf.
5. Interferometer for high precision orbit determination [online]. Available at http://adsabs.harvard.edu/full/ 2003ESASP.532E..39P.
6. Huang, Y., Hu, X., Zhang, X., Jiang, D., Guo, R., Wang, H., and Shi, S. (2011). Improvement of orbit determination for geostationary satellites with VLBI tracking. *Chinese Science Bulletin, 56 (26)*, 2765–2772.
7. Bushuev, F.I., Kaliuzhnyi, N.A., Slivinsky, A.P., and Shulga A.V. (2012). Determination of the range to geostationary telecommunications geostationary satellites using the signals of satellite television. *Radiofizika i Radioastronomia. 17 (3)*, 281–290 (in Russian).
8. Multilateration [online]. Available at http://encyclopedia.thefreedictionary.com/multilateration
9. Chernyak, V.S. (1993). *Multiposition Radiolocation*. Moscow: Radio i Sviaz (in Russian).
10. Hofmann-Wellenhof, B., Lichtenegger, H., and Collins, J. (1995). *Global positioning system: Theory and practice*. Kyiv: Naukova Dumka (in Ukrainian).
11. European Telecommunications Standards Institute. (1997). *Digital video broadcasting (DVB); Framing structure, channel coding and modulation for 11/12 GHz satellite services. European Standard (Telecommunications series). EN 300 421 V1.1.2 (1997-08)*. Sophia Antipolis: ETSI.

12. Cabot, R. (1981). A note on the application of the Hilbert transform to time delay estimation. *IEEE Trans. Acoust. Speech Signal Processing, (29) 3*, 607–609. DOI: 10.1109/TASSP.1981.1163564.
13. Trimble ThunderBolt E GPS Disciplined Clock. User Guide. [online]. Available at http://www.trimble.com.
14. GPS10RBN: 10 MHz, GPS Disciplined, Rubidium Frequency Standard. [online]. Available at http://www.ptsyst.com/GPS10R-B.pdf.

ĢEOSTACIONĀRA TELEKOMUNIKĀCIJU SATELĪTA POZĪCIJAS NEPĀRTRAUKTAS MONITORĒŠANAS REZULTĀTI, IZMANTOJOT DIGITĀLĀS SATELĪTTELEVĪZIJAS SIGNĀLA UZTVERŠANU DAŽĀDOS TELPAS PUNKTOS

F. Bušujevs, M. Kaļužnijs, J. Sibirjakova, O. Šuļga, S. Moskaļenko,
O. Balagura, Vl. Kuļišenko

K o p s a v i l k u m s

Rakstā sniegti ģeostacionārā telekomunikāciju satelīta «Eutelsat-13B» (13° austrumu garums) pozīcijas novērošanas rezultāti. Rezultāti iegūti, izmantojot radioinženierijas kompleksu, kuru veido četras digitālās satelīttelevīzijas signālus uztverošās stacijas Kijevā, Mukačevā, Harkovā un Nikolajevā, kā arī datu apstrādes centrs.

Katras stacijas aprīkojums, izmantojot GPS, ļauj sinhroni reģistrēt satelīttelevīzijas DVB-S signāla fragmentus uztvērēja kvadratūras detektora izejā. Kompleksie signāli tika saglabāti un, izmantojot Interneta savienojumu, nosūtīti uz datu apstrādes centru, kur uztverto signālu korelācijas apstrādes rezultātā trīs staciju pāriem tika noteiktas trīs lineāri neatkarīgas tiešā attāluma starpības *(Δr)*. Izmantojot multilaterācijas metodi, katrā sekundē izmērītās Δr vērtības tika transformētas satelīta Dekarta koordinātēs (XYZ) WGS84 koordinātu sistēmā.

Rakstā analizētas Δr, *X*, *Y* un *Z* laikrindas, kas iegūtas nepārtrauktos novērojumos laikposmā no 2015. gada marta līdz maijam. Viena *Δr*, *X*, *Y* un *Z* mērījuma kļūda ir atbilstoši 2,6 m, 3540 m, 705 m un 455 m. Izstrādātais komplekss tiek salīdzināts ar zināmiem analogiem. Apskatīti paņēmieni, kā samazināt satelīta koordinātu noteikšanas kļūdas.

Kompleksu var uzskatīt par ģeostacionāro telekomunikāciju satelītu pozīciju neatkarīgas uzraudzības sistēmas prototipu.

24.08.2016.

LATVIAN JOURNAL OF PHYSICS AND TECHNICAL SCIENCES
2016, N 5

DOI: 10.1515/lpts-2016-0032

USING CARBON-BASED COMPOSITE MATERIALS FOR MANUFACTURING C-RANGE ANTENNA DEVICES

N. Dugin[1,2], T. Zaboronkova[2,3], E. Myasnikov[4]

[1] Radiophysical Research Institute, 25/12a B. Pecherskaya Str., Nizhny Novgorod 603950, RUSSIA

ndugin@yandex.ru

[2] University of Nizhny Novgorod, 23 Gagarin Ave., Nizhny Novgorod 603950, RUSSIA

[3] R.E. Alekseev Technical University of Nizhny Novgorod, 24 Minina Str., Nizhny Novgorod 603950, RUSSIA

[4] Volga State University of Water Transport, 5a Nesterova Str., Nizhny Novgorod 603950, RUSSIA

C-range horn antenna made of a graphene-containing carbon-based composite material has been developed. Electrodynamic characteristics of the developed antenna and the identical metal antenna have been measured in the frequency range of 4.6–4.9 GHz. We have created two prototypes of horn antennas made of (i) carbon fiber and (ii) carbon fabric. It has been shown that the horn antenna made of graphene-containing composite material is capable of efficiently operating in the C-range frequency and possesses almost the same electrodynamic characteristics as the conventional metal antenna of the same geometry and size. However, the carbon-based antenna has enhanced stability in the wide range of temperatures to compare with the corresponding metal antenna.

Keywords: *composite materials, C-range frequency, electrodynamic antenna characteristics, graphene-containing carbon, horn antenna.*

1. INTRODUCTION

It is well known that carbon-based materials are widely used in aerospace and shipbuilding industry, and are considered promising in the future for antenna techniques. In the past decade, composite materials were mainly used for manufacturing the structural elements of microwave devices, which require improved durability. When using carbon materials for reflector antennas, the surface of antennas is covered by a materials containing metal particle for providing the electric conduction, which makes the antenna characteristics similar to those of the conventional metal prototypes. The use of composite dielectric metamaterials as elements of the waveguide or antenna systems (such as inserts, corrugated structures, coatings, etc.) can improve their reflection and scattering properties [1]–[3].

Despite a wide use of metamaterials in antenna techniques [3], little is known about the characteristics of microwave horn antenna made of carbon-based composite materials. Our studies have shown the possibility of using composite materials not only for manufacturing the elements of microwave devices, but also for creating antenna systems. We have already developed the prototypes of circular waveguide and horn antennas in microwave L-range (1.4–1.7 GHz) and shown that microwave antenna devices made of a graphene-containing carbon based material have almost the same characteristics as their metal analogues [4], [5]. In the present research we have created two prototypes of C-range horn antennas made of (i) carbon fiber and (ii) carbon fabric.

2. FORMULATION OF THE PROBLEM

It is the purpose of the present research to develop C-range horn antenna made of a graphene-containing carbon-based composite material. The devices based on carbon composite materials have a long lifetime, enhanced immunity to corrosion, the record-breaking durability-to-weight ratios, and high stability in a wide range of temperatures (see, e.g., [4], [6] and references therein). Note that the graphene-containing material properties depend on the concentration of a binding substance in the composite material [4], [7].

At first, we measured the conductivity of a carbon composite material containing graphene structures in the centimeter-wave range. The conductivity of such a material reached a value of 10^5 S/m [7]. As it is known, typical conductivity values for metals lie in the limits of 10^3–10^6 S/m. We also studied the polarization properties of the graphene-containing carbon composite material in the microwave range as a function of the concentration of the graphene structures. It was found that in the case of rotation of the composite-material thin plate by 90^0, the polarization coefficient with respect to the field amplitude amounted to about 20–30 %, depending on the concentration of a binding substance in the composite material [8]. Note, that the anisotropic properties of the composite materials may influence the radiation of electromagnetic waves from the carbon-based horn antenna, including such important characteristics as the radiation pattern, the antenna gain, etc.

To manufacture the prototype of C-range horn antennas made of carbon composite material, we used carbon fiber or carbon fabric and epoxy resin modified by graphene structures as a binding substance. It should be noted that we created two prototypes of horn antennas made of (i) carbon fiber and (ii) carbon fabric. The electrodynamic characteristics of both antennas were measured at a frequency of 5 GHz and compared with those of a conventional metal antenna of the same geometry and size.

It was shown theoretically and confirmed experimentally that for the waveguide of circular cross section made of a composite material with anisotropic property, the more efficient excitation of the H_{11} wave (or the H_{10} wave in a rectangular waveguide [9]) took place if the carbon fibers in the composite material of the waveguide walls lied in the plane perpendicular to the waveguide axis [4]. For the theoretical calculation of the composite antenna parameters, we used the model of a circular cross section waveguide with finite thickness of a wall. The waveguide is

immersed in a free space. It was assumed that the coductivity of the medium inside walls of the waveguide was described by a dielectric tensor with zero off-diagonal elements. Satisfying the continuity conditions for the tangential components on the boundaries of the waveguide walls we arrived at the equation for the eigenvalues of the waveguide. This equation allows us to estimate the geometrical parameters of the waveguide segment of C-range horn antenna. We obtained that the type of the fiber winding (longitudinal or transverse) was determined by the polarization of the antenna-excited electromagnetic field in the case of anisotropic conductivity of the walls. Further, we discuss some details of the manufacturing of horn antennas.

3. MANUFACTURING OF C-RANGE HORN ANTENNA

The horn antenna prototype contained the sequentially connected horn and segment of a circular waveguide, which were made of a graphene-containing composite material. During the manufacturing of the composite-material-based antennas, we used Zoltek Panex 35 (50K) carbon fiber (for the first prototype) and carbon fabric (for the second prototype) and the resin as binding substance, which was modified by graphene powder. The carbon fabric is a plain-weave of indicated carbon fiber. The structure of the carbon fiber and carbon fabric is shown in Fig.1. The size of unit cell of fabric is equal to 1.5cm × 1.5 cm. The conductivity of graphene-containing composite material depends on the binding substance. Note that the conductivity of composite material used for manufactoring of C-antenna is almost isotropic.

To manufacture the antenna, firstly we made blank matrix. The blank matrix was made from duralumin and had the external sizes exactly coinciding with the calculated geometric parameters of the device. Then we applied the required number of layers of the graphene-containing carbon fiber (or carbon fabric) to the external part of the blank using the transverse winding (Fig. 2). The thickness of the waveguide walls was determined by the necessary strength of the construction and approximately was equal to 3–5 mm. The blank matrix was separated from specimen after solidification of the antenna walls. The surface roughness of C-range antenna was less than $10^{-2}\,\lambda$. Thereafter removal of surface roughness of the antenna may be reached by the vacuum shaping. It is also worth noting that the process of manufacture of C-antenna is the same as L-antenna described in detail in [4], [5].

Fig. 1. Structure of the carbon fabric and the carbon fiber.

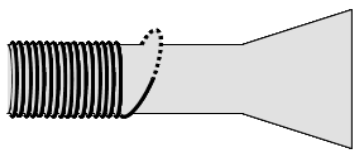

Fig. 2. Transverse winding of the carbon fiber to internal blank matrix.

As a result, we had the antenna prototypes made of the composite material. As an excitation device for the carbon-based antennas we used the analogous element of the metal antenna. Two orthogonal dipoles were used as excitation elements (Fig. 3).

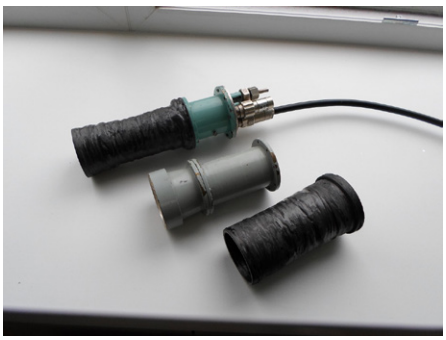

Fig. 3. Excitation elements.

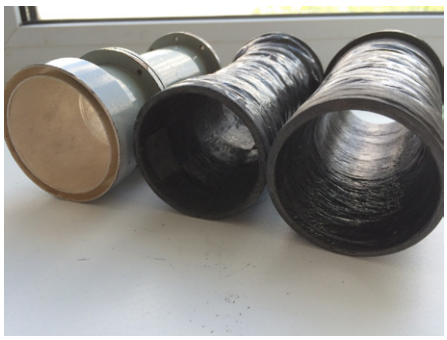

Fig. 4. View of the antennas made of metal (left), carbon fiber and carbon fabric (right, respectively).

The antennas made of carbon fiber and carbon fabric are shown on the right-hand side of Fig. 4, respectively. The geometry and structural features of the antenna prototypes were entirely identical to those of the metal antenna used for comparison with the carbon-based prototypes. The metal antenna is shown on the left-hand side of Fig. 4. As a result, the main characteristics of the manufactured antenna turned out to be almost identical to those of the metal antenna. Note that the creation of C-range antenna made of the graphene-containing carbon composite material and the study of its electrodynamic characteristics had been performed for the first time.

4. ELECTRODYNAMIC CHARACTERISTIC OF C-RANGE HORN ANTENNAS

The following electromagnetic parameters of the carbon-based antenna prototypes and metal antenna were measured: (i) the standing-wave ratio (Fig. 5), (ii) the amplitude-frequency response (Fig. 6) and (iii) the radiation pattern (Fig. 7). The measurements were performed by standard methods [10] under laboratory conditions without using an anechoic chamber. Receiving and transmitting antennas were located in the far zone relative to each other.

Figure 5 shows the standing-wave ratio (SWR) in the frequency range of 4.5–5.4 GHz for the antennas made of metal (5a, solid line and 5c), carbon fabric (5b, point line) and carbon fiber (5a, point line and 5d). It is seen in Fig. 5b that there is no essential difference between the corresponding measured values for the antennas made of carbon fiber and carbon fabric. It is seen in Fig. 5a that the dependences of SWR for carbon-based antennas are more smoothed than that of the metal antenna. It should be noted that the maximum (1.5) and minimum (1.2) values of the standing-wave ratio are approximately the same for all types of antennas.

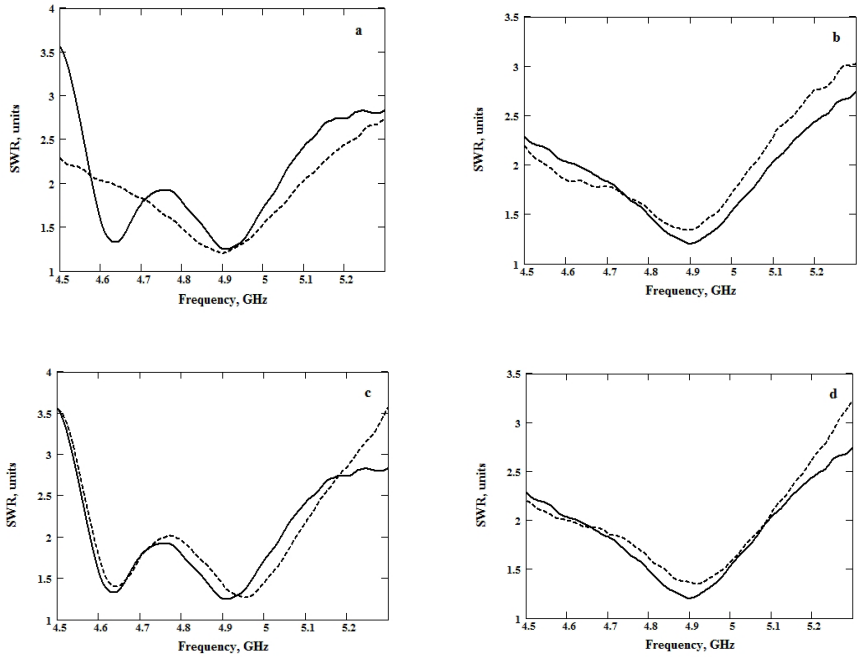

Fig. 5. The standing-wave ratio as a function of frequency for the antennas: a) made of the metal (solid line) and carbon fiber (point line) for the vertical field polarization; b) made of carbon fiber (solid line) and carbon fabric (point line) for the vertical field polarization, c) made of metal for the vertical (solid line) and the horizontal (point line) field polarizations, d) made of carbon fiber for the vertical (solid line) and the horizontal (point line) field polarizations.

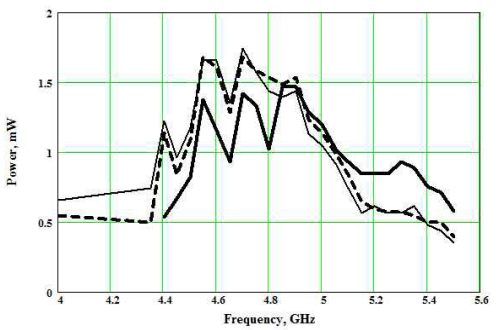

Fig. 6. The power of output signal as a function of frequency for the metal antenna (solid line), carbon fiber antenna (dashed line) and carbon fabric antenna (thin line).

The main antenna parameter is the gain, which characterizes the antenna efficiency, i.e., ohmic and radiation losses. The relative change of the antenna gains was measured by means of the amplitude-frequency response. Figure 6 shows the dependence of the power of the antenna output signal as a function of frequency for the metal antenna (solid line), carbon fiber antenna (dashed line) and carbon fabric antenna (thin line). It is seen that qualitative coincidence of all curves takes place. The sharp variations of curves in Fig. 6 are stipulated by peculiarities of excitation

devices and transmission antenna characteristics. The operating frequency of antennas may be determined as the range of 4.6–4.9 GHz.

The radiation pattern of antennas was measured at frequencies of 4.75 GHz and 5 GHz. Figure 7 illustrates the radiation patterns (main lobe) of the metal (dashed line) and carbon-based antennas (solid line) for the vertical polarization at a frequency of 4.75 GHz (Fig. 7a) and at a frequency of 5 GHz (Fig. 7b). For convenience, the measurement results for the main lobe of the radiation pattern of each antenna (circles or squares) were approximated by a Gaussian function (dashed or solid line).

It is seen in Fig. 7 that the difference between the corresponding measured values does not exceed 5 %, which is quite satisfactory for the laboratory tests. The main lobes of the radiation pattern of carbon fiber antenna and carbon fabric antenna practically coincide. Good agreement of all the measured quantities for the three antennas was observed. However, the distortion of radiation pattern (circles or squares) at a frequency of 4.75 GHz is more essential than at a frequency of 5 GHz. It was caused by conditions of laboratory measurements.

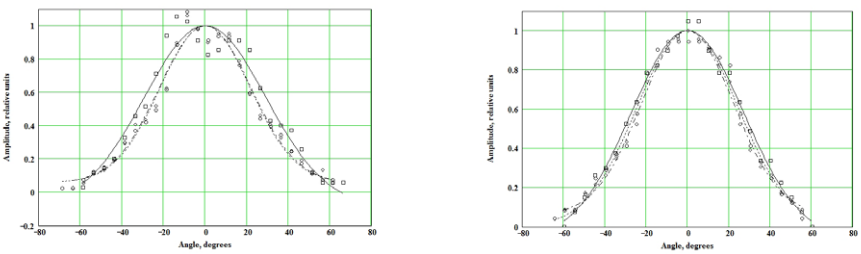

a) b)

Fig. 7. Radiation patterns of the metal antenna (dashed line) and carbon-based antenna (solid line): a) at a frequency of 4.75 GHz; b) at a frequency of 5 GHz. Circles (squares) correspond to the radiation patterns of the carbon-based antenna (metal antenna) without Gaussian approximation.

5. CONCLUSION

It has been shown that the C-range horn antennas made of carbon-based composite materials modified by the graphene structures are capable of efficiency operating and have almost the same characteristics as their metal analogue. We hope that in the future after improving the technology of the antenna manufacturing, the graphene-containing composite antenna devices will have substantial advantages over the metal analogues in terms of some key parameters (weight, temperature stability, durability, immunity to corrosion, etc.) and will be able to replace the conventional metal antennas.

ACKNOWLEDGMENTS

The authors gratefully acknowledge technical assistance of V. Chugurin. The present research has been supported by the Russian Science Foundation (project No. 14-12-00510).

REFERENCES

1. Zhigang, X., and Huiliang, X. (2009). Low refractive metamaterials for gain enhancement of horn antenna. *J. Infrared Millimeter Teraherz Waves*, *30 (2)*, 225–232.
2. Lashab, M., Hraga, H.I., Abd-Alhameed, R., Zebiri, C., Benabdelaziz, F., and Jones. S.M.R. (2011). Horn antennas loaded with metamaterial for UWB applications. *PIERS Online, 7 (2)*, 161–165.
3. Bychkov, I.V., Zotov, I.S., and Fedii, A.A. (2011). Studying microwave transmission and reflection in multilayer $CaSO_4$ $2H_2O$ – Graphite composites. *Technical Physics Letters*, *37 (7)*, 689 – 691.
4. Dugin, N.A., Zaboronkova, T.M., Myasnikov, E.N., and Chugurin, V.V. (2014). *Antenna-feeder the microwave oven the device from graphene-containing carbon composite material and its manufactoring.* Patent application №. 2014136727/28 — 2014-09-09.
5. Zaboronkova, T., Dugin, N., and Myasnikov, E. (2015). Microwave horn antenna made of a graphene-containing carbon composite material. *Proceedings of the 9th European conference on Antennas and Propagation* (EuCAP'2015). Lisbon, 2015. P. 7228220-1-7228220-2.
6. Rybin, I.V., Kuznetsov, P.A., Ulin, I.V., Farmakovskii, B.V., and Bakhareva, V.E. (2006). Nanomaterials structural and functional class. *Voprosu metallovedeniya*, *1 (45)*, 169 – 178 [in Russian].
7. Giboney, Kirk S. *Gap-mode waveguide*. Patent № WO2012128866 (A1) — 2012-09-27.
8. Dugin, N.A., Zaboronkova, T.M., Chugurin, V.V., and Myasnikov, E.N. (2013). Study of electromagnetic properties of multylayer graphene fractal structures by remote method. *The 21 annual International Conference on Advanced Laser Technologies (ALT 2013)*. P. 192.
9. Felsen, L.B., and Marcuvitz, N. (1973). *Radiation and scattering of waves*. Englewood Cliffs, USA: Prentice-Hall.
10. Tseitlin, N.M. (Ed.) (1985). *Methods of measurement of antenna characteristics*. Moscow: Radio I Svyaz' [in Russian].

OGLEKĻA KOMPOZĪTMATERIĀLU IZMANTOŠANA C JOSLAS ANTENU IZGATAVOŠANAI

N. Dugins, T. Zaboronkova, E. Mjasņikovs

K o p s a v i l k u m s

C diapazona rupora antenas tika izgatavotas no grafēnu saturošiem oglekļa kompozītmateriāliem. Tika mērīti šo antenu un analogas metāla antenas elektrodinamiskie raksturlielumi 4,6 – 4,9 GHz frekvenču diapazonā. Mēs izgatavojām divus rupora antenu prototipus: a) uz oglekļa šķiedru bāzes, b) uz oglekļa šķiedru auduma bāzes. Parādīts, ka grafēnu saturoša kompozītmateriāla rupora antena var efektīvi darboties C diapazona frekvencēs, un tās elektrodinamiskie raksturlielumi ir gandrīz vienādi ar tādas pašas ģeometrijas un izmēru metāla antenas raksturlielumiem, bet oglekļa kompozītmateriālu antena ir stabilāka par atbilstošu metāla antenu plašā temperatūru diapazonā.

24.08.2016.

LATVIAN JOURNAL OF PHYSICS AND TECHNICAL SCIENCES
2016, N 5

DOI: 10.1515/lpts-2016-0033

MEASUREMENTS OF INTERFEROMETER PARAMETERS AT RECEPTION OF GLONASS AND GPS SIGNALS

M. Nechaeva[1], D. Adamchik[2], Vl. Bezrukovs[3], N. Dugin[1,2], I. Shmeld[3], Y. Tikhomirov[1]

[1] Radiophysical Research Institute (NIRFI), 25/12a B. Pecherskaya Str., Nizhnij Novgorod, 603950, RUSSIA

[2] Lobachevsky State University of Nizhnij Novgorod (UNN), 23 Gagarin Ave., Nizhnij Novgorod, 603950, RUSSIA

[3] Engineering Research Institute "Ventspils International Radio Astronomy Centre" of Ventspils University College (VIRAC), 101 Inzenieru Str., Ventspils, LV-3601, LATVIA

The present paper deals with the calibration method of interferometers with antennas having a small effective area, on the quasinoise signals of GLONASS and GPS navigation satellites. Algorithms for calculation of antenna coordinates and instrumental delay from the analysis of correlation interferometer response to signals of satellites in the near field of the instrument were reviewed. The method was tested in VLBI experiments on interferometers with medium and large baselines that included radio telescopes of NIRFI and VIRAC. The values of the antenna coordinates and instrumental delay with an error within the limits of one discrete were obtained. The sources of measurement errors and ways to improve the accuracy of results were analysed.

Keywords: *baseline, calibration, data processing, delay navigation space satellites, VLBI.*

1. INTRODUCTION

Calibration of radio astronomical instruments, especially precision tools, such as Very Long Baseline Interferometry (VLBI), is a necessary procedure to ensure high accuracy of coordinate and time measurements. When using radio interferometers for solving astrometric, geodetic and astrophysical problems, the special attention is devoted to the high-precision measurements of the distance between the receiving antenna, i.e., baseline calibration, because errors in the baseline projections are directly included in errors of radiation source position or reference point location on the Earth's surface. As a rule, two problems are solved: direct problem, i.e., determination of the emission source coordinates from the known parameters of the interferometer, and inverse problem, i.e., the determination of receiving station coordinates from the known source location. Interferometric observations require

accurate measuring of the spatial delay, that is the difference between the time of signal arrival to the antennas of the interferometer. At instrument calibration, the component of the delay should be excluded, which is determined by clock mistiming on the stations, difference in the lengths of receiving channels, and so on, the so-called instrumental delay.

During the progress of VLBI technology, sufficiently effective methods of interferometer calibration [1], [2] were developed, but almost all of them involved the use of signals from extragalactic radiation sources (quasars, galaxies, and others) located at the "infinite" distance from the Earth and thus creating a flat front of the incident electromagnetic wave for all ground radio interferometric instruments. The discrete sources for given interferometer with sufficiently high intensity radiation are to be used for high-precision measurements. The selection of such sources is limited and high-quality calibration is carried out using antennas with a large effective area (with a mirror diameter of 15 meters and more). Traditional calibration method becomes inapplicable using radio telescopes of smaller diameters.

Putting into operation the global positioning systems in near-Earth space, a considerable number of satellites, which emit a powerful quasinoise signal, allow using small receiving antennas and are considered to be point sources for ground observers. In the case, when the sensitivity of interferometers is low, it is proposed to use the signals of GLONASS and GPS navigation space satellites (NSSs) as calibration sources for baseline measurement and instrumental delay, assuming that the coordinates of NSS are known with certain accuracy.

Calibration on NSS signals has some significant differences from the traditional interferometer calibration on extragalactic sources. One problem of measurement accuracy assessment is low precision (from the point of view of VLBI), at which the coordinates of NSS are known. Since NSSs are in the near field of the interferometer, the basic ratios should take into account the sphericity of the incident wave. A significant obstacle to achieving high accuracy for the delay measurement is a narrow frequency band of radiated GLONASS and GPS signals, thus requiring the use of mathematical and methodical methods to reduce error of the basic parameter measurement. It is also necessary to take into account that the spectrum of the NSS signals is quasinoise and the traditional procedure of primary processing for the noise signals requires correction.

Elaboration of interferometer calibration methods is a necessary preparatory task for solving the problem of measuring the space object coordinates, bearing in mind that the accuracy of the required value calculation in both problems depends on the accuracy of the delay and the interference frequency measurement.

2. EXPERIMENTS

In recent years, NIRFI and VIRAC have been carrying out joint experiments on different scientific tasks at VLBI-complex, comprising radio telescopes of small and medium diameter (Fig. 1) [3], [4], [5]. The first experiment on receiving of NSS signals with purpose to study the Earth's ionosphere was implemented in 2010 on the interferometer "Staraya Pustyn – Zimenki" with the baseline of 68 km. In 2012, the radio telescope RT-32 Irbene was involved in these experiments.

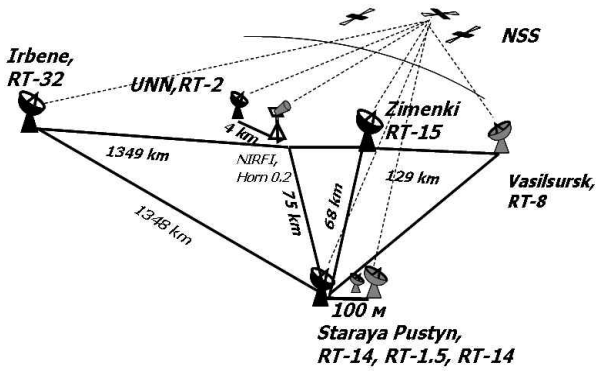

Fig. 1. VLBI-complex for the experiment on receiving of signals of navigation space satellites.

The experiments allowed accumulating an initial database, including the recording signals of NSS, on the basis of which the calibration method was tested. To calculate the interferometer parameters and verification capabilities of calibration on sources in the near field according to the developed algorithms, we used data of two experiments conducted in October of 2010 on the interferometer "St. Pustyn – Zimenki" and in September of 2012 on the interferometer "Irbene – Nizhny Novgorod State University (UNN) – St. Pustyn".

The main stages of the experiment are described briefly below. NSS signals received by antennas of the interferometer undergo cross-correlation processing, which consists of multiplying the signals with the preliminary compensation of time and frequency shifts. The delay is measured at the maximum of the correlation function and bears information about the calibration parameters, such as coordinates of the baseline and instrumental delay. Accordingly, the delay measurement is possible, when the signal emitted by the source has noise spectrum.

Figure 2 is an example of cross-correlation function obtained at reception of a signal from NSS 29601 GPS by the interferometer "St. Pustyn – Zimenki". Squares denote the values of the correlation function as a function of the delay for the single measurement. One discrete of delay measurements is inversely proportional to the sampling frequency, which in these experiments was 16 MHz at receiving bandwidth of 8 MHz. Discrete delay of 62.5 ns corresponds to one discrete in the definition of the difference between the propagation paths, which is equal to 18.7 m.

To clarify the position of the correlation function peak, we implemented an approximation of the data by a Gaussian function (solid line in Fig. 2), which describes well the maximum of cross-correlation function at reception of a noise signal in a rectangular frequency band.

Figure 3 shows the delay values depending on the time measured in the described manner. In this experiment, delay measurement was carried out with averaging time of 10 seconds at intervals with duration of 3 to 20 minutes, corresponding to the observation time of the satellite. A sequence of these values was interpolated by a polynomial function with calculation of errors. The result of the interpolation is shown in Fig. 3 by a solid line. For the given example the delay measurement error is 7.96 ns, which corresponds to an error determining the difference of propagation paths of signals 2.39 m.

Thus, application of the method allowed increasing the accuracy of the delay measurement nearly eightfold.

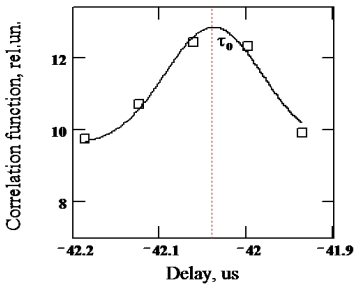

Fig. 2. Correlation function at receiving of signal of GPS 29601 at interferometer "St.Pustyn – Zimenki". October, 26, 2010. 09:30 UT. Boxes mark measured values, bold line denotes the approximated curve.

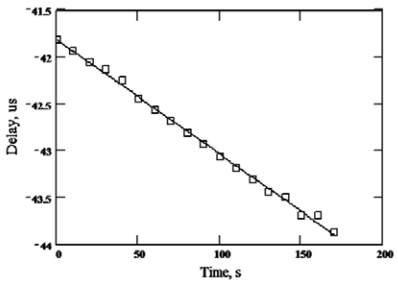

Fig. 3. Time dependence of delay obtained at receiving of signal of GPS 29601 at interferometer "St.Pustyn – Zimenki". October, 26, 2010. 09:30 UT. Boxes are the experimental values, bold line is a polynomial function approximating the data.

The delays measured this way were used to determine the parameters of the interferometer.

The dependence of the delay τ on the position vectors of VLBI-stations and instrumental delay $\Delta\tau$ is described by the equation:

$$\tau = \frac{1}{c}\left(\left|\mathbf{r}-\mathbf{R}_1\right| - \left|\mathbf{r}-\mathbf{R}_2\right|\right) + \Delta\tau\,, \qquad (1)$$

Here c is velocity of light in vacuum. Let us assume that known values are delay τ measured in the experiment and the geocentric vector $\mathbf{r}\{r_x, r_y, r_z\}$ describing the position of the satellite. Satellite coordinates were taken from the official website of GLONASS – Information-Analytical Centre of Federal Space Agency (https://www.glonass-iac.ru/archive/).

The unknown quantities in (1) are the geocentric vectors of radio telescopes $\mathbf{R}_1\{R_{1_x}, R_{1_y}, R_{1_z}\}$, $\mathbf{R}_2\{R_{2_x}, R_{2_y}, R_{2_z}\}$ and instrumental delay $\Delta\tau$.

Since NSSs are arranged in the near field of the interferometer, it is impossible to describe the dependence of the delay on the baseline coordinates by linear equation, as it is done in the traditional method of interferometer calibration on extragalactic radio sources. Thus, the coordinates of radio telescopes will be calculated, from which baseline parameters will be further obtained.

The number of equations increases the accuracy of the solution. As the number of measurements obtained in reviewed observations was little for the qualitative statistical evaluation, the task was simplified: it was assumed that the coordinates of one antenna were known. Thus, the task was reduced to finding the coordinates of the second antenna and instrumental delay.

We made calculations on the results of the experiment of 2010 measuring the delay from 9 NSSs on interferometer "St. Pustyn – Zimenki". Estimates of the coordinates of the antenna Zimenki at a given position of the antenna in the St. Pustyn are presented in Table 1.

The first column lists the coordinates of the antenna known from geodetic measurements and time shift between time scales in two different stations fixed during observations. The second column shows the results of calculations of the antenna coordinates and the instrumental delay and corresponding values of dispersion. The difference between the calculated parameters and the given values are displayed in the last column. As can be seen from the table, the discrepancy of antenna coordinates amounts to 2–4 meters and the dispersion is comparable in magnitude with an error of determination of the difference of signal propagation paths.

Table 1

Calculation of Antenna Coordinates in Experiment of 2010

Given parameters		Result of calculations and variance	Difference between the known and calculated values
R_{2x}, km	2549.035	2549.033 ± 0.009 km	2 m
R_{2y}, km	2486.162	2486.160 ± 0.011 km	2 m
R_{2z}, km	5274.220	5274.196 ± 0.018 km	4 m
$\Delta\tau$, mcs	16	16.894 ± 0.046 mcs	0.894 mcs

Thus, the differences of calculated and predetermined parameters are within the accuracy of delay measurement.

Despite the good results obtained on the middle baseline, the calculations made on the interferometers with large baselines "Irbene – UNN" and "Irbene – St. Pustyn", were unsatisfactory. The discrepancy between the known and calculated antenna coordinates significantly exceeded the expected values. It was necessary to perform the study of the causes, which touched all stages of solving the problem: the organization of the experiment, the procedure of processing and interpretation of results.

3. DISCUSSION

Following the analysis, two factors were revealed, which negatively affected the result of the calculation of the antenna coordinates in experiments at interferometers with large baselines.

Non-optimal schedule of observing session can be considered one of the reasons of the decrease in accuracy. For calculation of the baseline parameters, it was necessary to use the data of experiment on the study of artificial ionospheric turbulence at radio sounding by NSS signals. In this experiment, the antennas received the signals from the satellites located in a narrow sector of angles in azimuth, in the direction of the heating facility "Sura" acting on the ionosphere [6]. Such arrangement of NSSs relative to VLBI baselines is not optimal for the calibration of the interferometer, because the best accuracy is achieved at regular distribution of sources on the celestial sphere. In addition, part of the measurements used in the calculations was made on one satellite and disturbed the condition of equation independence. Most errors were also associated with insufficient number of measurements for the statistical analysis.

A solution to this problem consists in the modification of the experiment schedule, which will provide the choice of NSS in a wide range of angles. It is necessary to reduce the time of observation of one satellite to 5–10 minutes and to increase the number of independent measurements.

The second and the most important factor in the loss of accuracy is a large error when measuring the delay. If the averaging time at the correlation was 10–30 seconds in the experiment with the middle baseline, then in the experiment with large baselines the averaging time was reduced to 1 second in order to evaluate the impact of the ionosphere on the passing signals in short time intervals. The small averaging time led to a large spread of delays. In addition, failures of synchronization of recording system were detected.

Figures 4a and 4b show examples of graphs of the difference between the measured and calculated delay for the two satellites observed on the interferometer "Irbene – UNN". One step of delay change corresponds to one discrete of 62.5 ns. Approximation of the maximum of the correlation function to clarify its position was not performed.

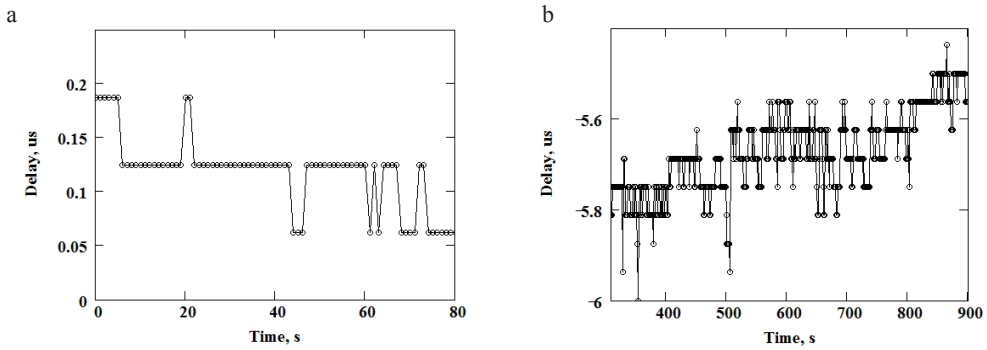

Fig. 4. Difference between the calculated and experimental delay depending on time at observation on interferometer "Irbene – UNN". September, 5, 2012.

(a) – GPS 29601, 10:45 UT; (b) – GPS 28474, 09:35 UT.

To improve the accuracy of the delay measurement, it is necessary to increase the frequency reception bandwidth to the maximum possible, i.e., to the bandwidth of the signal emitted by the satellite. The signal band of GLONASS satellites is 10 MHz, and that of GPS is 20 MHz. The discrete of delay is equal to 50 and 25 ns, respectively. It is necessary to use the mathematical methods for the accurate measurement of delay in maximum of the correlation function as it was done in the experiment with the small baseline. This way will allow increasing the accuracy of the delay measurement by several times.

To sum up, it should be noted that the experimental verification of the calibration method of the interferometer on signals of NSSs showed the possibility to measure the coordinates of the receiving stations of the interferometer with an accuracy of 2–4 m, which was a good result considering that the NSS coordinates were known for limited accuracy. The results of the analysis of the revealed problems will be taken into account in future research and will allow improving the accuracy of the method for calibration of interferometers with large baselines.

ACKNOWLEDGMENTS

The present research has been supported by the Ministry of Education and Science of the Russian Federation and Russian Foundation for Basic Research (project No. 13–02–00586-a).

REFERENCES

1. Schuh, H., and Behrend, D. (2012). VLBI: A fascinating technique for geodesy and astrometry. *Journal of Geodynamics, 61,* 68–80, DOI 10.1016/j.jog.2012.07.007.
2. Thompson, A.R., Moran, J.M., and Swenson, G.W. (2001). *Interferometry and synthesis in radio astronomy*. Second Edition. New York: Wiley.
3. Dugin, N.A., Nechaeva, M.B., Antipenko, A.A., Dement'ev, A.F., and Tikhomirov, Yu.V. (2011). Measurement of antenna parameters by signals from space satellites of the GLONASS and Navstar navigation systems. *Radiophysics and Quantum Electronics, 54 (3)*, 159–165.
4. Dugin, N., Antipenko, A., Bezrukovs, Vl., Gavrilenko, V., Dementjev, A., Lesins, A., Nechaeva, M., Shmeld, I., Snegirev, S., Tikhomirov, Yu., and Trokss, J. (2013). Radio interferometric research of ionosphere by signals of space satellites. *Baltic Astronomy, 22 (1),* 25–33.
5. Nečajeva, M., and Šmelds, I. (2015). VLBI pētījumi VeA IZI VSRC no 2010. līdz 2014. gadam. *Ventspils Augstskolas Inženierzinātņu institūtam VSRC 20. Ventspils Augstskola, 2015, ISBN 978-9984-648-55-2*, *246-260 (in Latvian)*.
6. Belikovich, V.V., Grach, S.M., Karashtin, A.N., Kotik, D.S., and Tokarev, Yu.V. (2007). The "Sura" facility: Study of the atmosphere and space (a review). *Radiophysics and Quantum Electronics, 50 (7),* 497–526.

INTERFEROMETRU PARAMETRU MĒRĪJUMI, IZMANTOJOT GLONASS UN GPS SIGNĀLUS

M. Ņečajeva, D. Adamčiks, Vl. Bezrukovs, N. Dugins,
I. Šmelds, J. Tikhomirovs

K o p s a v i l k u m s

Aplūkota interferometru ar maza efektīvā laukuma antenām kalibrēšana, izmantojot sistēmu GLONASS un GPS pavadoņu signālus, kuru raksturlielumi ir līdzīgi trokšņu raksturlielumiem. Apskatīti radiointerferometru punktu koordināšu un iekārtās radušos signāla aizkavēšanos aprēķina algoritmi, izmantojot interferometra atsauci uz satelītiem tā tuvajā zonā. Metode pārbaudīta VLBI eksperimentos ar vidēju un lielu bāzu interferometriem, kuru sastāvā bija VSRC un Krievijas Radiofizikas institūta Nižņijnovgorodā radioteleskopi. Iegūtas antenas koordinātu un aparatūras izsaukto signāla aizkavju vērtības ar precizitāti līdz aizkaves diskretizācijas kvanta daļām. Analizēti kļūdu avoti un rezultātu precizitātes uzlabošanas iespējas.

24.08.2016.

LATVIAN JOURNAL OF PHYSICS AND TECHNICAL SCIENCES
2016, N 5

DOI: 10.1515/lpts-2016-0034

PHYSICAL AND TECHNICAL ENERGY PROBLEMS

THE DEVELOPMENT OF NANOTECHNOLOGIES AND ADVANCED MATERIALS INDUSTRY IN SCIENCE AND ENTREPRENEURSHIP: SOCIOECONOMIC AND TECHNICAL INDICATORS. A CASE STUDY OF LATVIA (PART TWO)

I. Geipele[1], S. Geipele[1], T. Staube[1], G. Ciemleja[1], N. Zeltins[2]

[1] Institute of Civil Engineering and Real Estate Economics,
Faculty of Engineering Economics and Management,
Riga Technical University,
6-210 Kalnciema Str., LV-1048, Riga, LATVIA
Email: Ineta.Geipele@rtu.lv
[2] Latvian MemberKommitte of World Energy Council,
Latvian Academy of Sciences,
Akadēmijas laukums 1, Rīga, LV 1050, Riga, LATVIA

Part two of the in-depth scientific study clarifies the significant social and technical indicators of the development of nano-field at the macro, micro, and meso development levels of the economic environment in Latvia in the framework of the given theme. The analytical assessment of numerical change in socioeconomic and technical factors clearly demonstrates the interaction of nano-field with the development of science and manufacture, as found out in the study. The identified indicators are proposed to use for research, comparison and implementation in any other country of the world.

Keywords: *advanced materials, development of science, economic environment level, engineering economic indicator system, nanotechnologies, research.*

1. INTRODUCTION

The development of nano-field mainly depends on the interaction between science and entrepreneurship, where the country's socioeconomic as well as legal and political situation is particularly important. Technology and innovation development in Latvia points to the formation of scientific and business potential. According to the results of the current scientific research, the analysed development process is determined by a variety of indicators.

To reach the aim of the study the current part of work has the following tasks: (1) to make comparison of the socioeconomic and technical indicators found with

that of other countries if applicable; (2) to generate the data according to the levels of the economic environment; (3) to provide remarkable recommendations for the responsible parties.

2. ASSESSMENT OF THE SOCIAL AND TECHNICAL INDICATORS

Social Indicators

Although a significant impact on the development of nano-field is exerted by economic indicators, social data play no less important role. Quality of life is the well-being index of particular members of society, which includes the life satisfaction level in the family and society as well as material support. Thus, the material well-being of population is closely related to the economic development of a particular country. Therefore, at the macro or global level in the social indicator group the authors put forward life satisfaction, subjective well-being, median equivalised disposable income, GINI coefficient, human development index, and GNP per capita.

Life satisfaction as a component of subjective well-being indicator results from the survey of population, who had to answer the question "All things considered, how satisfied are you with your life as a whole these days?" on a 10-point scale from 1 "dissatisfied" to 10 "satisfied" and based on the data of Real and Dobewall's (2011) study, in the early 1990s after Latvia regained its independence the indicator was around 5.8 [23], while experiencing significant fluctuations in the twenty-year period in 2015 the mean estimated result of this indicator remained approximately at the same level – about 6.0 [24]. According to the analysis performed for the period of 1998–2014, in Latvia the life satisfaction index is 5.52 compared with Estonia that has reached a higher level or 6.16 and Lithuania – 5.84. The index in Latvia is similar to that in Egypt – 5.52, India – 5.51 and Belarus – 5.53. However, according to the 2014 research data by the Organisation for Economic Co-operation and Development (OECD), which was not yet joined by Latvia and Lithuania, Estonian inhabitants measured life satisfaction at a 5.6 grade. "That is one of the lowest scores in the OECD, where average life satisfaction is 6.6". Greece, Hungary, Portugal and Turkey have also less than average life satisfaction grade [25].

Lonska (2013), studying the Latvian subjective well-being indicators, found out that in the period of 2000–2010 compared to the Baltic neighbours, Latvia took the lowest position together with Lithuania. This means that the average happiness level of Latvian population is assessed by 5.3 points ("0" – the lowest score, "10" – the highest score), the average happiness level of Lithuanian population is 5.5 points, but Estonian people value their happiness with 6.0 points out of 10 possible [26], [24]. Taking into account the previously analysed economic indicators and the subsequent analysis, the authors will also prove the hypothesis of the study performed by Lonska (2013) that states that subjective well-being of Latvian population depends not only on the volume of GDP per capita, but also on factors such as unemployment rate and income inequality [26], which in the authors' present study will substantiate Latvia's low position in the subjective well-being index.

An important role is also played by the median equivalised disposable income indicator, which characterises the poverty/wealth level of society and reflects the available income trends. It is used to analyse savings conditions and purchasing power for a particular year in absolute terms and to compare the dynamics in the period for cumulative changes in real and nominal values, by population structure and income levels, as well as to determine the relative median income ratio [27]. According to Eurostat data for the period of 2008–2012, the negative cumulative change in median equivalised disposable income was experienced by Greece and Iceland, i.e., more than 34 % and 23 % fall, respectively. Latvia was the third country in the EU by negative changes of this indicator in the reporting period, i.e., around 20 % below zero, which was followed by Croatia -16.2 %, Spain and Ireland around -5 %. In Hungary, these changes were much smaller -8 %; in Lithuania and Cyprus they were the same, i.e., -12 %. The highest positive changes of the indicator were recorded in Norway, Slovakia, Switzerland, Sweden and Poland [27].

Taking into account the Latvian negative result of median equivalised disposable income index, Gini coefficient that characterises income inequality perfectly matches the analysis above. According to Eurostat data, Latvia (35.5) together with Bulgaria (35.4) shared the 1st and 2nd place in terms of the polarisation degree of the EU society – they had the highest Gini coefficient in 2014 [28]. This means that the disposable income of Latvian prosperous households is growing more and more rapidly than that of other countries, thus demonstrating the high degree of polarisation of society.

Human development index refers to human development achievement in three dimensions – a long and healthy life, knowledge and a decent standard of living. In 2013, this index was 0.81 in Latvia and it was ranked 48th out of 187 countries of the world; similar results were demonstrated by Cuba, Kuwait, Croatia and Argentina [29]. The authors consider that for Latvia this figure is quite satisfactory and appropriate, as in Latvia it is possible to adopt healthy lifestyle, studying at educational institutions is available at reasonable prices and public life standards are not yet at risk.

On a global scale, well-being of Latvian population may also be determined by GNP per capita as GNP covers income belonging to residents of a particular state, including income from economic activities performed by particular country's citizens abroad. Performing the analysis, the authors have found out that the World Bank has attributed Latvia to the high-income non-OECD group of countries, which means that Latvia is ranked among the high-income countries. The World Bank data show that in 2013 the Latvian GNP per capita accounted for 15,280 US dollars; by this indicator Latvia took the 47th position out of 176 countries of the world. A little bit better situation was characteristic of countries such as Estonia, Slovakia, Oman, Uruguay, but quite similar results with Latvia were demonstrated by Chile and Lithuania in 2013 [30]. However, the authors conclude that, despite the World Bank's high rating, both economic and social indicators analysed above indicate a not-so-good situation in terms of social welfare, which shows that in Latvia in the area of income inequality and administration there are still a lot of challenges ahead.

At the meso or national level, in accordance with Fig. 2 presented in Part 1 of the scientific research [31], the authors have included the employment and unemployment rate in the country, reflecting the country's economic activity dynamics.

According to Eurostat data for the period of 2014, in Latvia 884.6 thsd people were employed, taking into account the resident population concept and age group from 15 to 64 years [32], of which 318.7 thsd employees or 36 % of the total number of employees had higher education (the specialisation sector is not indicated) in the 4th quarter of 2014 [33]. In South Korea, one of the leading countries in the nano-field, in 2013 the number of researchers per million people was 6,457, in Latvia – 1,802, very close to the number of researchers in Poland (1,851), Bulgaria (1,693) and Italy (1974). By comparison, in Lithuania this figure is about 2,900, in Estonia – 3,340 [34]. The given number of researchers in Latvia is related to low growth of R&D, which is analysed in the economic indicator group, and to inadequate salary level of researchers in Latvia. However, according to Eurostat data, in 2014 Latvia among all EU member states had a high unemployment rate of 10.8 % [35] and, in accordance with the database of the Central Statistical Bureau of Latvia, the total number of unemployed in Latvia accounted for 99.6 thsd people [36], which was a relatively high indicator, because the total population of Latvia was 1,990,351 in 2014 [37]. It is also worth mentioning that in Europe the unemployment rate of more than 10 % is characteristic of the following countries: Lithuania, Bulgaria, Ireland, France, Slovakia, Portugal, Italy, Croatia, Cyprus, Spain and Greece. The mentioned problems in Europe can be explained by political and economic factors, such as the Greek crisis, aggravate relations with Russia and alarming extent of the refugee influx in Europe. With regard to the employment and unemployment rate in the nano-field, the authors explain that unfortunately in Latvian statistics there is not freely available information, and the information available at databases is quite general – compiled by age group, education and ethnicity.

Despite worries about the consequences of the rise of unemployment rate, by continuing development of innovative technologies [38], it is known that in the nano-field there is demand for highly qualified specialists. Consequently, in terms of unemployment by educational attainment, in Latvia the average number of unemployed with higher education was 16.5 % of the total number of unemployed in 2014 [39], according to the State Employment Agency data at the beginning of 2015 almost 15 % of unemployed were specialists with higher education [40].

To be able to precisely determine the development of nano-field in science in Latvia, the authors put forward the following parameter at the meso level: number of specialists trained at vocational education institutions in the field of nanotechnology. According to the data by the Ministry of Education and Science of Latvia, from 2000 to 2011 approximately 58 % of secondary school graduates continued studies at universities and colleges. Industry representatives expressed a demand for specialists in engineering (23 % of respondents) and manufacturing technologies (15 % of respondents), while in 2011, 21 % of students majored in engineering and natural sciences. The largest number or more than 50 % of students studied at programmes related to social sciences, business and law in 2011 that demonstrated potential obstacles to non-compliance of labour demand and supply. The greatest human resource provision in engineering and technological sciences belongs to materials sciences – 25 % and to biotechnology – 2 %. According to the number of doctoral theses defended in Latvia, the number of specialists in engineering accounts for about 13 % of the total number of young scientists in the period of 2000–2013 [41].

As a last social indicator at the meso level, the authors have chosen the public and private social spending share of GDP, which is an important indicator of social protection and security in any country's economy. According to Eurostat data for 2012, the expenditure on social protection in Latvia was the lowest among the EU member states, and it accounted for only 14.0 % of GDP [42]. Compared with Latvia, the average EU expenditure on social protection is 29.1 % of GDP, which demonstrates that in Latvia social protection and security are not developed.

At the micro or business level, in the social indicator group it is worth noting the experts' average monthly salary level in the nano-field according to qualification. With regard to this indicator, the aggregated statistical information in Latvia was not available to the authors, but during the survey carried out by the authors it was found out that also in Latvia specialists working in the nano-field comprised highly qualified professionals who depending on their company's remuneration policy were appropriately motivated. However, in order to clarify the data from the official sources of information available, it is worth mentioning that as of December 2014 professional, scientific and technical services staff received the average monthly salary of 963 EUR gross, scientific research staff – 1,301 EUR gross and personnel working in the education system – 675 EUR gross [43].

By comparison, in Germany an average monthly salary is 2,290 EUR in teaching/education, while in science and technical services – 3,686 EUR. In Lithuania, in the teaching/education category an average monthly salary is 756 EUR, while in Poland – 747 EUR [44], which demonstrates that in the Latvian education system employees receive a relatively low salary in the EU. In turn, "U.S. salaries for nanotechnology engineering technicians range from $ 30,000 to $ 94,000" per year or according to other sources, the average annual salary is $ 79,000 [45].

The authors have also found out that one of the reasons that hinders the development of research in Latvia is human resources problem: a too small number of people employed in science and the lack of renewal potential. There is a lack of motivation and the ability to attract young professionals to scientific and academic activities. A serious cause for the lack of interest in research is compared to other EU countries: low salary levels and limited career opportunities at research institutions [46]. The problem of the average monthly remuneration in Latvia also complements the situation of the large number of unemployed with higher education. At present, there are situations when people tend to retrain, take positions in other sectors or at all go abroad just because of a poor salary level in Latvia, thus demonstrating the importance of this social indicator, i.e., it is crucial to make residents in their own country feel valued and safe.

Technical Indicators

At the macro or global level, in technical indicator group there are the following innovation development indicators: number of patents in the nano-field per year: nanotechnology patents in EPO, USPTO, German Patent Office (DPMA); nanotechnology patent applications published in EPO, USPTO, German Patent Office (DPMA). At the website of nanoscience statistics, in the section of nanotechnology patents in EPO Latvia is ranked 62nd out of 67 countries, presenting one patent per

year from 2010 to 2014, except for 2012 when no patent was granted [47]. By comparison, in Ukraine in 2012 and 2013 one patent was granted every year, in 2014 – none; in Estonia and Cyprus in 2014 – one patent, but as of June 2015 – 2 patents; in Croatia and Romania in 2014 and June 2015 – 1 patent every year; in Egypt and Algeria in 2014 – one patent to each country. With regard to nanotechnology patents in the USPTO, Latvia was ranked 57th out of 67 countries, although in the period from 2010 to June 2015 Latvia did not have any patent registered in the USPTO [48]. In the specified time period, no patent was presented by Serbia, Algeria, and Uzbekistan. By comparison, Latvia's neighbour Estonia was ranked 54th in this report, presenting 5 patents in 2013, 6 patents in 2014 and 1 patent as of June 2015, while the other neighbour Lithuania was ranked 46th – with 2 patents in 2013, 4 patents in 2014 and 1 patent as of June 2015. The same situation for Latvia can be observed in the section of nanotechnology patents in the German Patent Office (DPMA) – no patent in the period from 2010 to 2015. Here it should be noted that many countries (67 countries) do not have a patent in this report. The best indicators in this report are demonstrated by Germany, the USA and Japan [49].

In the first group of technical indicators, a better situation is experienced by Latvia in terms of nanotechnology patent applications published in EPO, which means that the nanotechnology patent applications were published (but not yet granted) in EPO. According to this report, as of June 2015 Latvia was ranked 16th out of 67 countries, presenting 17 patents, which meant a very significant increase because in 2014 there was only one patent and in 2013 – 3 patents [50]. However, it is too early to speak about the positive development of nanoscience, since in other nanoscience statistical sections Latvia does not demonstrate such high rates, and a level of public funding for research and innovation is still low in Latvia. This is demonstrated by the next analysis on nanotechnology patent applications published in USPTO, where Latvia took the last position out of 67 countries [51]. By contrast, the analysis of data on nanotechnology patent applications published in the German Patent Office (DPMA) indicates that the patenting activity is very low in the German region, as well as in Iran, Bulgaria, Lithuania and many other countries; and Latvia also did not have patent applications in this section during the period from 2010 to 2015 [52].

As a last indicator of the technical indicator group at a global level, there is the ratio of nanotechnology patents to nano-articles, where Latvia took the last position out of 67 countries [53]. The above-mentioned analysis of patent types confirms that, unfortunately, at present in Latvia research, technological development and, in particular, innovation infrastructure are underdeveloped, as well as commercialisation activities are weak compared with mean indicators of other countries, but a report on nanotechnology patent applications published in EPO points to a positive "take-off", which suggests that Latvia has potential in this area.

At the meso or national level, in the technical indicator group the authors have included indicators such as production volume, structure and dynamics, as well as science-based product sales volumes. It is worth noting that in 2012 Ltd. GroGlass was attributed to a large and medium-sized commercial group in Latvia. The high-tech factory GroGlass is one of five companies in the world that is able to produce glass with anti-reflective nano-coating. Being the youngest – established in the 21st century, GroGlass is the only one manufacturer that can cover technologically glass

from both sides simultaneously. The glassed artwork in the Louvre and National Gallery of London – Bang&Olufsen TV displays – these are just a few examples of diverse opportunities and outstanding quality of non-reflective glass manufactured in Latvia [54].

As a last indicator at the meso level, it is worth mentioning the nanotechnology transfer infrastructure efficiency (incubators, parks, prototyping laboratories, pilot plants, technological development and competence centres, clusters), which is an important technology transfer and innovation infrastructure development indicator and points to the development of necessary environment for new technology development and research result commercialisation. Taking into account the fact that the Latvian nanotechnologies, intelligent materials industry and science have historically evolved quite significantly and in a timely manner, for example, "by establishment of the vacuum metallization design bureau and later production of vacuum coating systems" in the early 1960s, and in the early 1990s working on the "concept of the development of the technology centres" [55], or development of nuclear physics starting from the 1950s [56], there are separate scientific developments and areas that still continue developing or have already been sold and then patented in other countries, or the infrastructure is relatively outdated and operates with low capacities and requires new investment. Therefore, the authors conclude that in terms of nanotechnology transfer infrastructure Latvia just undergoes the stage of development, as demonstrated by NanoTechEnergy cluster [57], Space Technology cluster activities [58] and metalworking cluster development [59]. Latvian entrepreneurs, especially small and medium-sized enterprises, and scientists cannot implement the technology transfer stage that is important for innovation process before the product is ready for production, because there is no technology transfer infrastructure and there is a lack of instruments to attract researchers to manufacturing enterprises [46]. According to the informative report by the Ministry of Education and Science of Latvia, in 2011 a number of "separate clusters were established, for example, in such fields as electronics, chemistry, pharmaceutics, space technology and logistics; however, their added value was unclear. Latvia has undertaken the first modernisation attempts by establishing nine research centres of national importance, but it seems that they are disproportionately much more focused on academic science" [41].

At the micro or business level, the technical indicator group includes three subgroups: the number and capacity of qualitative laboratories, capacity and power of technology and equipment, sufficiency of resources; qualitative indicators of existing product development and processing: the effect from improvement, nanomaterial characteristics; number of patent applications published in the nano-field, number of patents sold in the nano-field.

According to the report of the Ministry of Education and Science of Latvia, "the knowledge base is fragmented and degraded, including research, technological development and, in particular, innovation infrastructure is underdeveloped. As a consequence, there are an extremely low number of spinoffs, as well as start-ups based on the developments made in the public research sector" [41]. Some manufacturing companies in the nano-field consider that they have "strong internal capacities such as more experience in the use of the high technologies, higher ability to increase the capacities of production and level of the salaries" [31]. However, the above-

mentioned set of indicators (the number and capacity of qualitative laboratories, capacity and power of technology and equipment, sufficiency of resources) is very important, as it provides information on the provision of infrastructure of local market manufacturers. These data should be clarified for separately organised targeted study, as each sub-sector of nano-field could have its own requirements. Thus, in the survey conducted by the authors it has been found out that 75 % of the Latvian innovative multifunctional material manufacturers have their own laboratories, 14 % use outsourcing services, and the same number of responses has been received by companies who do not use laboratories at all.

Qualitative indicators of existing product development and processing – the effect from improvement, nanomaterial characteristics – are essential indicators that indicate to what extent the goal set by technology use or innovative material development has been achieved, for example, ratios of different types of efficiency measured by: degradation [60], encapsulation [61], thickness of the coating and dependence on external actions [62], use of resources [63], [64], time [65], [66], and other efficiency measures depending on the type of the nanotechnology or nanomaterial and goal of research.

With regard to the number of patent applications published in the nano-field, which has already been analysed at the macro level, the authors consider that this indicator is also important at the micro level, as well as the number of patents sold in the nano-field or copyright transfer should be clarified by organising the targeted study, for example, by a direct survey method. This would provide valuable facts about the country of origin of the invention, which is not reflected at the official databases at least in relation to Latvia.

3. FURTHER RESEARCH

The authors will continue to collect and aggregate data from primary and secondary sources and improve the developed engineering economic indicator system in terms of other indicator groups: scientific, legal, political, ecological, health and safety, information and communication, and management implementation levels and indicators.

4. CONCLUSION

1. Analysis of the types of patents confirms that Latvia is ranked among the less active countries in terms of commercialisation of inventions and, unfortunately, at present in Latvia research, technology development as well as innovation infrastructure, in particular, are underdeveloped and weak in comparison with mean indicators of other countries. It is possible to quite distinctly observe the target markets of Latvian manufacturers in the nano-field: primarily – the EU and for individual companies – the United States.
2. Publicly available information on the development of nano-field in Latvia, the most influencing socioeconomic and technical indicators in the Latvian specific macroeconomic context allow concluding that the nanotechnology and advanced materials industry are still developing slowly in Latvia and for its proper iden-

tification separate target studies should be organised in order to obtain missing analytical information.

3. In Latvia, at the national level it is necessary to make conceptual solutions in order to promote cooperation among science, research and business, as well as the parties' own activity and interest in mutual cooperation and support are of importance.

REFERENCES

1. Realo, A., & Dobewall, H. (2011). Does life satisfaction change with age? A comparison of Estonia, Finland, Latvia, and Sweden. *Journal of Research in Personality, 45 (3)*, 297–308. DOI: 10.1016/j.jrp.2011.03.004
2. Veenhoven, R. (n.d.). *Happiness in Latvia* (LV), World Database of Happiness, Erasmus University Rotterdam. The Netherlands. Retrieved 14 January 2016, from http://world-databaseofhappiness.eur.nl
3. Better life index. (n.d.). OECD. Retrieved 6 January 2016, from http://www.oecdbetterlifeindex.org/topics/life-satisfaction/
4. Lonska, J. (2013). Comparative analysis of subjective well-being of Latvia`s inhabitants in the context of economic development of the Baltic States. *Latgale National Economy Research, 1 (5),* 148–166. DOI: 10.17770/lner2013vol1.5.1157.
5. Living standard statistics – median equivalised disposable income. (n.d.). Eurostat. Retrieved 6 January 2016, from http://ec.europa.eu/eurostat/statistics-explained/index.php/Living_standard_statistics_-_median_equivalised_disposable_income
6. Gini coefficient of equivalised disposable income. (n.d.). Eurostat. Retrieved 11 January 2016, from http://ec.europa.eu/eurostat/tgm/table.do?tab=table&language=en&pcode=tessi190
7. World Rankings – Human Development Index. (n.d.). World Data Atlas. Retrieved 10 November 2015, from http://knoema.com/atlas/topics/World-Rankings/World-Rankings/Human-Development-Index
8. GNI per capita, Atlas method (current US$). (n.d.). The World Bank. Retrieved 10 November 2015, from http://data.worldbank.org/indicator/NY.GNP.PCAP.CD/countries?order=wbapi_data_value_2014%20wbapi_data_value%20wbapi_data_value-last&sort=asc&display=default
9. Geipele, I., Geipele, S., Staube, T., Ciemleja, G., Zeltins, N., & Ekmanis, J. (2016). The development of nanotechnologies and advanced materials industry in science and entrepreneurship: Socioeconomic and technical indicators. A case study of Latvia (Part One). *Latvian Journal of Physics and Technical Sciences* (53), 4, 3–13, DOI: 10.1515/lpts-2016-0023.
10. Employment (main characteristics and rates) – Annual averages. (n.d.). Eurostat. Retrieved 19 December 2015, from http://appsso.eurostat.ec.europa.eu/nui/submitViewTableAction.do
11. Economically active population by education level and gender on a quarterly basis. (n.d.). Central Statistical Bureau of Latvia. Retrieved 10 November 2015, from http://data.csb.gov.lv/pxweb/lv/Sociala/Sociala__isterm__nodarb/NB0030c.px/table/tableViewLayout1/?rxid=d543db7b-f122-4e1f-aced-7a7707fd86e7 (in Latvian)
12. Researchers in R&D (per million people). (n.d.). The World Bank. Retrieved 5 January 2016, from http://data.worldbank.org/indicator/SP.POP.SCIE.RD.P6?order=wbapi_data_value_2013+wbapi_data_value&sort=asc

13. Unemployment rate by sex and age groups – Annual average, %. (n.d.). Eurostat. Retrieved 10 January 2016, from http://appsso.eurostat.ec.europa.eu/nui/show.do?wai=true&dataset=une_rt_a
14. The Number of employed and unemployed aged 15–74 years by gender on a monthly basis, seasonally adjusted data. (n.d.). Central Statistical Bureau of Latvia. Retrieved 10 January 2016, from http://data.csb.gov.lv/pxweb/lv/Sociala/Sociala__isterm__nodarb/NB00010m.px/table/tableViewLayout1/?rxid=d543db7b-f122-4e1f-aced-7a7707fd86e7 (in Latvian).
15. Latvia – Population. (n.d.). Country Economy. Retrieved 13 November 2015, from http://countryeconomy.com/demography/population/latvia
16. Bainbridge, W. S. (Ed.). (2007). Nanotechnology: Societal implications: I: Maximising benefits for humanity; II: Individual perspectives. *Springer Science & Business Media*. Netherlands.
17. The unemployed by sex and educational level on a quarterly basis (n.d.). Central Statistical Bureau of Latvia. Retrieved 10 January 2016, from http://data.csb.gov.lv/pxweb/lv/Sociala/Sociala__isterm__nodarb/NB0200c.px/table/tableViewLayout1/?rxid=d543db7b-f122-4e1f-aced-7a7707fd86e7 (in Latvian).
18. Statistical portrait of unemployed person. (2015). State Employment Agency. Retrieved 10 January 2016, from http://nva.gov.lv/index.php?cid=6&mid=494&txt=495&t=stat (in Latvian).
19. About development of smart specialisation strategy (2013). Ministry of Education and Science of Latvia. Retrieved 13 January 2016, from http://tap.mk.gov.lv/mk/tap/?pid=40291636 (in Latvian).
20. File:Expenditure on social protection, 2002–12 (% of GDP) YB15.png. Eurostat Statistics Explained. Retrieved 13 January 2016, from http://ec.europa.eu/eurostat/statistics-explained/index.php/File:Expenditure_on_social_protection,_2002%E2%80%9312_%28%25_of_GDP%29_YB15.png
21. Average monthly salary by activity types / per month (EUR). (n.d.). Central Statistical Bureau of Latvia. Retrieved 14 January 2016, from http://data.csb.gov.lv/pxweb/lv/Sociala/Sociala__isterm__dsamaksa/DS0040m_euro.px/table/tableViewLayout1/?rxid=-89fa53c2-5ff7-456f-aae4-c4274cf3b2aa (in Latvian).
22. Salary survey in Germany, Lithuania and Poland. (n.d.). Salary Explorer 2015. Retrieved 14 January 2016, from http://www.salaryexplorer.com/salary-survey.php?loc=81&loctype=1
23. Nanotechnology Careers. (n.d.). National Nanotechnology Infrastructure Network. Retrieved 9 January 2016, from http://www.nnin.org/news-events/spotlights/nanotechnology-careers
24. Science, Technology Development and Innovation Guidelines for 2014–2020. Riga, 2013, Regulations of the Cabinet of Ministers No. 685 as of 28 December 2013. Retrieved 5 January 2016, from https://www.google.com/url?sa=t&rct=j&q=&esrc=s&source=web&cd=3&ved=0CCwQFjACahUKEwjKz-6H8JnIAhXIjSwKHR6JDDo&url=http%3A%2F%2Fwww.innovativelatvia.lv%2Ffiles%2Finov%2Fcontent%2FZinatnes_tehnologijas_attistibas_un_inovacijas_pamatnostadnes_2014.%2520%25E2%2580%2593%25202020.gadam_.doc&usg=AFQjCNHBPccjrOxlMiOlbZKAYbPQt-i4rA&sig2=ck17B0cnEsUJlhtzYGWG7g&cad=rja (in Latvian)
25. Nanotechnology patents in EPO (Patent). (n.d.). StatNano. Retrieved 15 December 2015, from http://statnano.com/report/s95
26. Nanotechnology patents in USPTO (Patent). (n.d.). StatNano. Retrieved 15 December 2015, from http://statnano.com/report/s89

27. Nanotechnology patents in German patent office (DPMA) (Patent). (n.d.). StatNano. Retrieved 15 December 2015, from http://statnano.com/report/s97
28. Nanotechnology published patent applications in EPO (Patent). (n.d.). StatNano. Retrieved 15 December 2015, from http://statnano.com/report/s96
29. Nanotechnology published patent applications in USPTO (Patent). (n.d.). StatNano. Retrieved 15 December 2015, from http://statnano.com/report/s78
30. Nanotechnology published patent applications in German patent office (DPMA) (Patent). (n.d.). StatNano. Retrieved 15 December 2015, from http://statnano.com/report/s98
31. Ratio of nanotechnology patents to nano-articles (Patents per 100 articles). (n.d.). StatNano. Retrieved 20 December 2015, from http://statnano.com/report/s88
32. Project BIRTI Science, Technology and Innovation Strategy for Smart Specialisation for 2014–2020. Riga, 2013. Association "Baltic Institute of Research, Technology and Innovation" (BIRTI). Retrieved 14 January 2016, from https://www.google.lv/?gws_rd=ssl#q=Projekts+BIRTI+Zin%C4%81tnes%2C+tehnolo%C4%A3iju+un+inov%C4%81cijas+strat%C4%93%C4%A3ija+lietprat%C4%ABgai+specializ%C4%81cijai+2014.-2020.gadam (in Latvian)
33. Staube, T., Ciemleja, G., & Geipele, I. (2014). The origins of nanotechnology in Latvia. *Advanced Materials Research*, *1025–1026*, 1083–1087. DOI: 10.4028/www.scientific.net/AMR.1025-1026.1083.
34. Ekmanis, J., Gavars, V., Mikelsons, K., Tomsons, E., & Zeltins, N. (2010). Development of nuclear energetics in Latvia. In the 21st World Energy Congress, 12–16 September 2010 (16 pp.). Montreal, Canada: World Energy Council. Retrieved from http://www.indiaenergycongress.in/montreal/library/pdf/18.pdf
35. NanoTechEnergy. (n.d.). Association "Baltic Institute of Research, Technology and Innovation" (BIRTI). Retrieved 20 January 2016, from http://www.birti.eu/en/what-we-do/item/81-nanotechenergy
36. Ventspils High Technology Park (2012). *Strategy of Space Technology and Services Cluster 2012-2015.* Retrieved 20 January 2016, from http://www.vatp.lv/ (in Latvian)
37. Cluster Project. (n.d.). Association of Mechanical Engineering and Metalworking Industries. Retrieved 24 January 2016, from http://www.masoc.lv/aktivitates/projekti/klastera-projekts (in Latvian).
38. Thangavel, S., Thangavel, S., Raghavan, N., Krishnamoorthy, K., & Venugopal, G. (2016). Visible-light driven photocatalytic degradation of methylene-violet by rGO/Fe3O4/ZnO ternary nanohybrid structures. *Journal of Alloys and Compounds*, *665*, 107–112. DOI: 10.1016/j.jallcom.2015.12.192
39. Badran, H. A., Ajeel, K. I., & Lazim, H. G. (2016). Effect of nano particle sizes on the third-order optical non-linearities and nanostructure of copolymer P3HT:PCBM thin film for organic photovoltaics. *Materials Research Bulletin*, *76*, 422–430. DOI: 10.1016/j.materresbull.2016.01.005
40. Stodola, P., Jamrichova, Z., & Stodola, J. (2012). Modelling of erosion effects on coatings of military vehicle components. *Transactions of FAMENA*, *36 (3)*, 33–44.
41. Wolden, C. A., Abbas, A., Li, J., Diercks, D. R., Meysing, D. M., Ohno, T. R., et al. (2016). The roles of ZnTe buffer layers on CdTe solar cell performance. *Solar Energy Materials and Solar Cells*, *147*, 203–210. DOI: 10.1016/j.solmat.2015.12.019.
42. Zhang, X., Tang, Z., Hu, D., Meng, D., & Jia, S. (2016). Nanoscale p–n junctions based on p-type ZnSe nanowires and their optoelectronic applications. *Materials Letters*, *168*, 121–124. DOI: 10.1016/j.matlet.2016.01.044.

43. Martínez, I. A., Roldán, É., Dinis, L., Petrov, D., Parrondo, J. M. R., & Rica, R. A. (2015). Brownian Carnot engine. *Nature Physics*, *12 (1)*, 67–70. DOI: 10.1038/nphys3518.
44. Yardimci, N.T., & Jarrahi, M. (2015). 3.8 mW terahertz radiation generation through plasmonic nano-antenna arrays. In 2015 IEEE Int. Symposium on Antennas and Propagation & USNC/URSI National Radio Science Meeting, 19– 24 July 2015 (pp. 2113–2114). Vancouver, Canada: IEEE. DOI: 10.1109/APS.2015.7305446.

NANOTEHNOLOĢIJU UN VIEDO MATERIĀLU INDUSTRIJAS ATTĪSTĪBA ZINĀTNES UN UZŅĒMĒJDARBĪBAS JOMĀS: SOCIĀLEKONOMISKIE UN TEHNISKIE RĀDĪTĀJI. LATVIJAS PIEREDZE (OTRĀ DAĻA)

I. Geipele, S. Geipele, T. Štaube, G. Ciemleja, N. Zeltiņš

K o p s a v i l k u m s

Padziļinātā zinātniskā pētījuma otrajā daļā publikācijas tēmas ietvaros tiek noskaidroti Latvijā nozīmīgākie nano jomas attīstību raksturojošie sociālie un tehniskie indikatori makro, mikro un vidējā ekonomiskās vides attīstības līmeņos. Sociālekonomisko un tehnisko rādītāju skaitlisko izmaiņu analītiskais vērtējums skaidri pierāda nano jomas mijiedarbību ar zinātnes un ražošanas attīstību, kā tas konstatēts pētījumā. Identificētie indikatori tiek piedāvāti pētījumiem, salīdzināšanai un izpildei jebkurā citā pasaules valstī.

24.08.2016.

LATVIAN JOURNAL OF PHYSICS AND TECHNICAL SCIENCES
2016, N 5

DOI: 10.1515/lpts-2016-0035

ENERGY PRODUCTION FROM BIOGAS: COMPETITIVENESS AND SUPPORT INSTRUMENTS IN LATVIA

G. Klāvs, A. Kundziņa, I. Kudrenickis,

Institute of Physical Energetics, 21 Aizkraukles Str., Riga, LATVIA
e-mail: energy@edi.lv

Use of renewable energy sources (RES) might be one of the key factors for the triple win-win: improving energy supply security, promoting local economic development, and reducing greenhouse gas emissions. The authors ex-post evaluate the impact of two main support instruments applied in 2010-2014 – the investment support (IS) and the feed-in tariff (FIT) – on the economic viability of small scale (up to $2MW_{el}$) biogas unit. The results indicate that the electricity production cost in biogas utility roughly corresponds to the historical FIT regarding electricity production using RES. However, if in addition to the FIT the IS is provided, the analysis shows that the practice of combining both the above-mentioned instruments is not optimal because too high total support (overcompensation) is provided for a biogas utility developer. In a long-term perspective, the latter gives wrong signals for investments in new technologies and also creates unequal competition in the RES electricity market. To provide optimal biogas utilisation, it is necessary to consider several options. Both on-site production of electricity and upgrading to biomethane for use in a low pressure gas distribution network are simulated by the cost estimation model. The authors' estimates show that upgrading for use in a gas distribution network should be particularly considered taking into account the already existing infrastructure and technologies. This option requires lower support compared to support for electricity production in small-scale biogas utilities.

Keywords: *biogas, electricity production, energy production price, investment subsidies, feed-in tariff.*

1. INTRODUCTION

Taking into account the contribution of renewable energy sources (RES) not only to the reduction of greenhouse gas (GHG) emissions but also to enhancing energy security and promoting national economy, the extensive use of RES is one of the energy policy priorities in the EU on the whole and in Latvia, in particular. It is essential to meet the GHG emissions reduction target within both the EU 2020 Climate and Energy Package and the new EU 2030 Framework for Climate and Energy [1].

Today Latvia is definitely on the way of reaching the RES 2020 target (at least 40 % of the total gross final energy consumption (GFEC) from renewables);

namely, in 2014 the renewable energy accounted for 38.65 % of the total GFEC [2], according to the latest data, it amounted to ~172 PJ [3]. Regarding the contribution of different RES to total renewable energy, solid biomass accounted for 77.85 %, hydroenergy (normalised for annual variation) – 16.40 %, biogas ranked third with 3.60 %. As far as the RES target components are concerned, in 2014 the share of renewable energy was 52.19 % in heating and cooling (planned in 2020 – 59.8 %), 51.09 % in electricity consumption (planned in 2020 – 53.4 %) and only 3.23 % in transport (planned in 2020 – 10 %) [2].

Thus, we see that the RES ratio is high in the electricity sector. In the period of 2010–2015, RES capacity in Latvia grew by ~10 % (from 1622 MW_{el} to 1784 MW_{el}) and 30 % of this increase was related to biogas technologies. The total electrical capacity of biogas technologies has increased from 11 MW_{el} (2010) to 60 MW_{el} (2015), and it is mainly due to actively introducing biogas technologies in the agriculture sector [4].

Although electricity produced from biogas for the time being still makes up a small fraction (~5 %) of the electricity consumed, a variety of benefits might be reached owing to biogas utilisation. The issue under consideration should be the sustainability of national biogas policy allowing for the implementation of biogas capacities without the negative side effects such as exaggerated support to biogas and the risk of market distortion.

The policy implemented in Latvia in the 2007–2013 planning period provided that the electricity producer who used biogas could receive both the feed-in tariff (FIT) and the support investment within the framework of the national Rural Development Programme (RDP) [5] co-financed by the European Agricultural Fund for Rural Development. The simultaneous availability of both support instruments vitally promoted the implementation of biogas technologies in the agriculture sector. In 2014, biogas production reached 3.136 PJ, including biogas produced in the agriculture sector – 2.688 PJ, landfill gas – 0.355 PJ and sewage sludge gas – 0.093 PJ (for comparison, in 2008 the production of all types of biogas was only 0.369 PJ). In 2015, 49 biogas plants with the total capacity of ~50 MW_{el} operated in the agriculture sector, which, within the procedure of FIT, sold to the national grid ~316.5 GWh renewable electricity [6]. Thus, the average electrical capacity of single biogas plant operating in the agriculture sector in Latvia is relatively high ~1MW_{el}, being in the interval of 0.21–2.4 MW_{el}. To compare, in Germany the average electrical capacity of biogas plant in the agriculture sector is ~330 kW_{el} [7]. In the Latvian situation, biogas plants, largely developed as a separate activity of the agriculture sector, are mainly based on the use of dedicated energy crops for biogas fermentation. It has caused significant increase of areas sown under maize: in 2011–2015 the areas sown under maize have more than doubled (in 2005 – 2.9 thsd ha, in 2011 – 11.3 thsd ha, in 2015 – 25.6 thsd ha) [8].

At present, new rights to sell electricity through the FIT programme are not being granted and a topical issue is the development of new legislation for promoting renewable electricity that ensures compliance with the principles set in the Communication from the European Commission 2014/C200/01 [9]. The research below presents an ex-post evaluation of the Latvian support scheme in relation to biogas production development and effective utilisation of it both from private investors'

point of view and optimal use of state resources. To determine the optimal support for promoting biogas production, a cost estimation model has been simulated both for on-site production of electricity and upgrading to biomethane for use in a low-pressure gas distribution network.

2. FEED-IN TARIFFS FOR BIOGAS ELECTRICITY

Two Regulations of the Latvian Cabinet of Ministers (CMR) provide for the application of FIT for the existing plants. Out of all biogas plants operating in the agriculture sector, 30 (total electrical capacity ~30.5 MW_{el}) operate under the CMR regarding electricity production utilising RES [10] and 19 (total electrical capacity ~19 MW_{el}) operate under the CMR regarding electricity production in combined heat-power (CHP) mode [11].

The Regulations [10] determined FIT depending on unit capacity: $FIT = 188 \cdot k$ for the first 10 years after starting the operation of the unit (k - differentiating coefficient, varies within the range from 1.24 for units with electrical capacity of 0.08 MW_{el} and to 1.008 for units with electrical capacity of 2 MW_{el}); for the next 10 years FIT is decreased by 20 % ($FIT = 188 \cdot k \cdot 0.8$).

In the case of [11], the FIT depends both on unit capacity and the end-user natural gas tariff T_g approved by the Public Utilities Commission, $FIT=(T_g \cdot k / 9.3) \cdot 4.5$. T_g depends directly upon the purchase price of natural gas (PPNG) at the border [12] and it is different for different groups of end-users depending upon the consumption volume of natural gas. The Amendments of [11], adopted in August 2013, introduced the 10-year limit for FIT application. This provision will be in force from 1 January 2017. It can be concluded that the instability of FIT due to the dependence on natural gas price turned out to be one of the main disadvantages, e.g., in the period of October 2008 – April 2014 the highest and lowest PPNG differed more than twice [13]. The Amendments of [11], adopted in April 2014, introduced the maximum value of PPNG applied for FIT calculation – 277.46 EUR/1000 m^3.

The biogas plants operating in the agriculture sector were launched after 2010 and in compliance with the above CMR they would maintain their rights still for a long time. To find a legally correct solution for optimising the present FIT scheme and avoid overcompensation, in 2014 the Subsidised Electricity Tax Law was adopted [14]. In the summer 2016, the Cabinet of Ministers adopted new Amendments to both CMRs introducing a special coefficient to avoid overcompensation as well as revoked the link with the end-users' natural gas tariff. The evaluation presented in this article is based on the FIT support scheme prior to the adoption of these Regulations.

3. METHODOLOGY OF ASSESSMENT

The calculated costs of biogas produced in the agriculture sector set the basis for the objective of the research, which is to find the most competitive and for the state support most efficient solution for biogas use. The research presents a comparative analysis of two solutions: 1) on-site production of electricity and (2) upgrading

to biomethane for use in a low-pressure gas distribution network. The methodology is based on the mathematical modelling and analysis of key parameters determining the price of biogas and the produced end product.

Investment cost, raw material cost and operation cost are taken into account in the calculation of biogas production costs. Investment cost and operation cost (Table 1) are based on average values, which are obtained from analysing the information about biogas technologies used in Latvia and other European countries [15]–[22]. The calculation is performed for a 10-year period; the IRR for the period is 10 %. The algorithm is provided to calculate both the costs of biogas volume and electricity production for the capacities of 250 kW_{el}, 500 kW_{el}, 1000 kW_{el} and 2000 kW_{el} of an electricity generation utility (internal combustion engine).The utility annual operation is presumed to be 7000 hours.

The model proceeds on the assumption that biogas is produced from dedicated energy crops, primarily maize, and the cost of this raw material in Latvia is 25 EUR/ton [23]. The assumed cost of the raw material is slightly lower than that used in calculations in other EU countries, where it ranges between 31–35 EUR/ton (e.g., [8], [15]).

When assessing on-site production of electricity, in the modelling only the income from electricity sales, according to FIT, is taken into account, but not the income from the sale of thermal energy. Such an approach is due to the limitations in the use of thermal energy.

When assessing upgrading to biomethane for use in a low-pressure gas distribution network, the model presumes that the investment cost for building the gas pipeline and necessary connection [24] amounts to average 1000 EUR/m and in all cases the gas pipeline is built of equal length (500 m).

Table 1

Assumptions of Technical and Financial Data for Biogas Equipment

Installed electrical capacity, MW_{el}	0.25	0.50	1.00	2.00
	Biogas production equipment			
Specific investments, 1000 EUR/MW_{el}	3785	2990	2590	2290
Specific annual operational costs, 1000 EUR/MW/year	670	626	603	593
	Internal combustion engine			
Specific investments, 1000 EUR/MW_{el}	946	747	647	498
Specific fixed operational costs, 1000 EUR/ MWh	25	25	25	25
	Biogas upgrading to biomethane facility			
Specific investments, 1000 EUR/MW_{el}	1765	1395	1210	1070
Specific fixed operational costs, 1000 EUR/ MWh	12.7	10	8.7	7.7

FIT values are calculated according to the formulae above as defined in CMR [10] and [11]. It is essential to compare FIT values and electricity market price. According to the Nord Pool Spot information, in 2015 the average electricity market price in the Latvian price region was 41.8 EUR/MWh. Figure 1 clearly reveals that the FIT value was essentially, about 3–4 times, higher than the electricity market price.

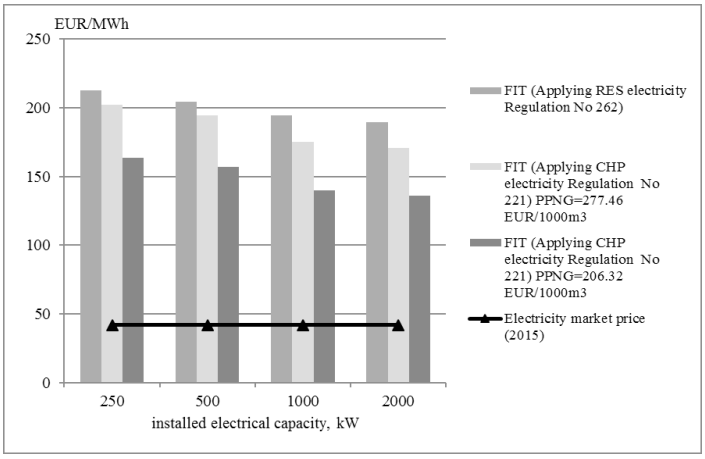

Fig. 1. Comparison of feed-in tariff and electricity market price: a case of Latvia.

4. RESULTS AND DISCUSSION

At first, the biogas production cost was compared with the price of natural gas for end-users with the annual consumption within the range of 1.26–12.6 Mm^3 that corresponded to the installed electricity generating utility with the capacity of 0.7–7 MW_{el}. Figure 2 reveals that the cost of biogas produced in the agriculture sector is high, and the difference is most outspoken with the biogas production equipment of smaller capacity.

In its turn, the biogas production equipment that ensures the required volume of biogas for 2 MW_{el} electricity generating utility is the approximate margin when the production cost of unpurified biogas and the price of natural gas for end-user become comparable upon the condition that PPNG is ~327 EUR/1000m^3. If PPNG is 277.46 EUR/1000 m^3 (corresponds to the maximum PPNG value in the FIT calculation, see above), the biogas production cost also in such 2 MW_{el} biogas production utility considerably exceeds (for more than 7 EUR/MWh) the price of natural gas for the end-user.

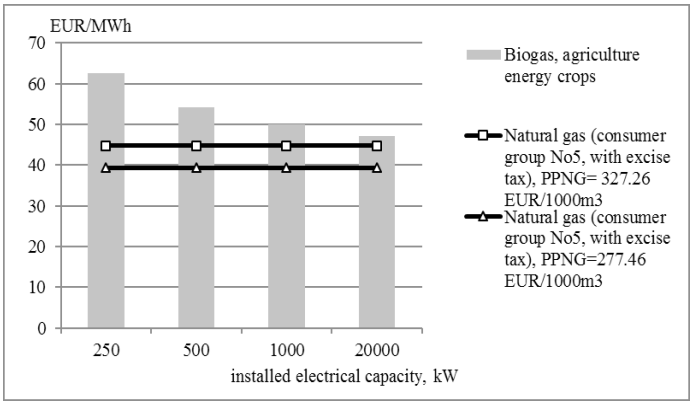

Fig. 2. Comparison of biogas costs, produced from agricultural energy crops, and natural gas end-use tariff.

Figure 3 provides the comparison of the upgraded to biomethane biogas production cost with the above-mentioned price of natural gas for end-users. It reveals that for low-scale plants the production cost of upgraded to biomethane biogas per 1 MWh is considerably higher, as well as the specific costs (per 1 MWh) are considerably higher for the connection to a natural gas network.

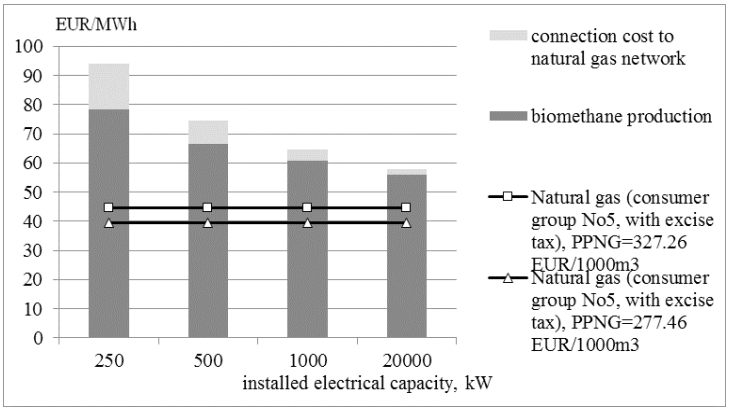

Fig. 3. Comparison of biogas cost, produced from agricultural energy crops and upgraded to biomethane for use in low-pressure gas distribution network, and natural gas end-use tariff.

In the final stage of the research, the electricity generation cost at a biogas plant and FIT values were compared. Figure 4 describes the situation if FIT is the only applied support instrument. The following conclusions may be drawn from the modelling results:

RES electricity [10] FIT value exceeds electricity generation cost at biogas plants with the electrical capacity above 1000 kW_{el}, at the capacity of 500 kW_{el} the electricity generation cost and FIT are practically the same; however, electricity generation cost at low-scale (~250 kW_{el}) biogas plants is higher than RES electricity FIT.

CHP electricity [11] FIT value, calculated at the highest historically PPNG=327 EUR/1000 m^3, considerably exceeds electricity generation cost at biogas plants with the electrical capacity above 500 kW_{el}, but does not exceed at low-scale (~250 kW_{el}) biogas plants. When setting limitations for CHP electricity FIT, the calculated FIT value at PPNG=277.46 EUR/1000m^3 is lower than electricity generation cost at all biogas plants of all the described range of capacities.

The modelled results clearly notify of a critically different situation if the owner of biogas equipment had a chance to use the RDP investment support [5] and sell electricity under FIT. Figure 5 compares FIT values with the modelled electricity generation cost at a biogas plant that has received the maximum 40 % of investment support. The following conclusions may be drawn from the modelling results:

Using RES electricity under FIT, support to biogas plants exceeds the generation cost by 25–40 EUR/1 MWh, depending upon the installed electrical capacity (the higher the capacity, the greater the difference between the generation cost and FIT).

Even at the set PPNG limitations for CHP electricity FIT, the calculated FIT value (at PPNG=277.46 EUR/1000m^3) exceeds the generation cost by 25–27 EUR/MWh.

Consequently, it implies that in the case of combined support (investment support and FIT) when FIT values considerably exceed electricity generation cost the intensity of the applied support mechanism is too high.

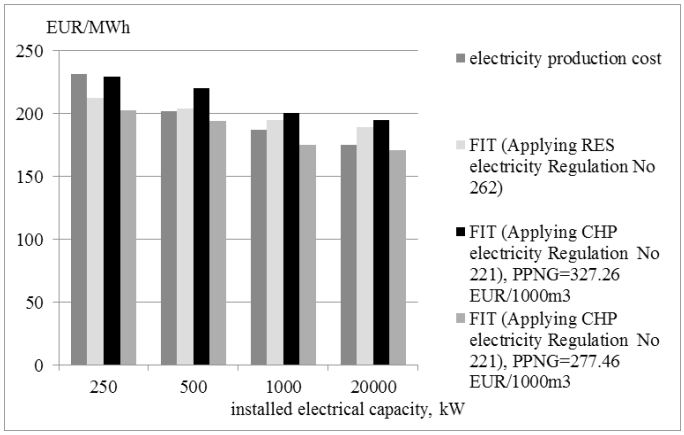

Fig. 4. Comparison of electricity production cost (without investment support) and feed-in tariffs.

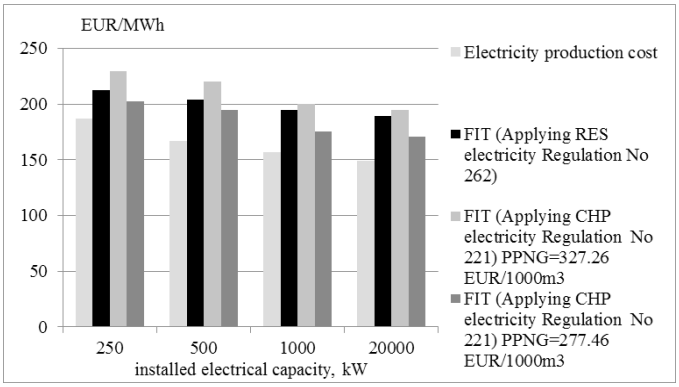

Fig. 5. Comparison of electricity production cost (with additional investment support 40 %) and feed-in tariffs.

When assessing the economic basis for different ways of biogas use, the calculation was performed for two options to find out the difference between: (1) electricity generation cost at biogas plants and electricity short-term marginal cost at natural gas CHP (condensing mode), (2) upgraded biogas cost and natural gas end-users' price (at PPNG=277.46 EUR/1000m^3) both expressed as fuel components for the generated electricity with effectiveness ratio of 55 %; investment support were not considered in the present research.

Figure 6 reveals the necessary support for each of the ways of biogas use. It shows that smaller subsidies are necessary for biogas upgrade to biomethane for use in a low-pressure gas distribution network than for electricity generation at small-scale biogas plants. When analysing the results, it should be taken into account that this upgrading may require bigger subsidies if the biogas plant is located farther

away from the natural gas network and larger investments are needed for building a longer gas pipeline. If the natural gas price drops, the subsidy amount increases for injecting biogas in a natural gas network.

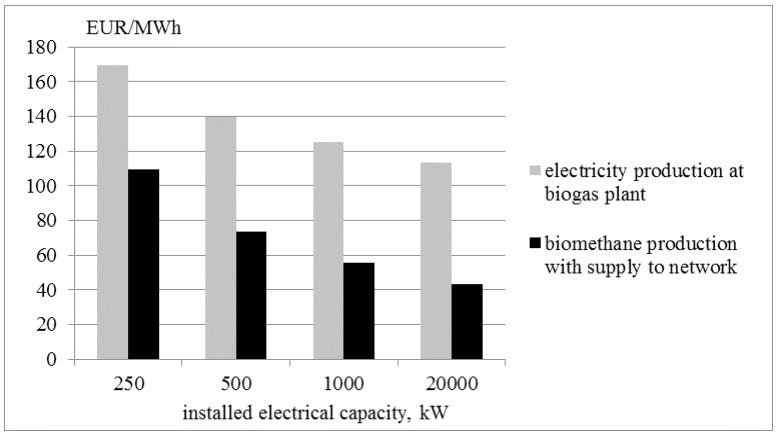

Fig. 6. Estimated necessary support per unit of produced electricity for different ways of use depending upon the capacity of the biogas utility.

5. CONCLUSIONS

The results show that the modelled price of electricity providing economic viability of electricity producing biogas utility in the agriculture sector is significantly higher than the average electricity market price. This causes the necessity to apply a support mechanism in order to facilitate the introduction of biogas electricity technologies.

In case electricity is generated at low-scale (up to 2 MW_{el}) biogas utilities and feed-in tariff (FIT) is the only support instrument, then the electricity generation cost at biogas utilities is approximately that of the FIT provided for in Cabinet of Ministers Regulation No. 262. At a high natural gas price (PPNG = 327.26 EUR/1000m^3), the FIT in accordance with Cabinet of Ministers Regulation No. 221 was also approximately that of electricity generation cost at a biogas utility. If the natural gas price drops, the FIT is insufficient for covering electricity generation cost at a biogas utility.

The analysis of FIT and investment support policy in Latvia revealed that the application of both these instruments was unbalanced and provided unreasonably high support for biogas utility developers. Such an unbalanced policy of too high subsidies sends wrong signals to long-term investments in new technologies, causes unequal competition in the RES electricity market and eventually creates problems to justify the RES policy to the society.

Supporting electricity generation at small-scale (up to 250 MW_{el}) biogas utilities, a compromise should be found between the economy-dictated development of projects with a larger capacity and the development of small-scale projects, which better correspond to the local needs.

At present, maize constitutes most of raw material for biogas production in Latvia, but in the future more attention should be devoted to the use of manure and manufacturing waste.

The research shows that in terms of biogas utilisation development, biogas upgrading for further injection in a natural gas network is more profitable with regard to the state support as it requires smaller amount of support. Considering the requirements provided for by the Directive on the deployment of alternative fuels infrastructure (2014/94/EU), further assessment, additional to the above, is necessary to assess the economic viability of upgraded biogas use in the transport sector.

Undoubtedly, also in the future in Latvia the use of biogas will be an important component of RES, climate policy and regional development. Consequently, a sustainable support mechanism of this resource is to be developed, which takes into account the interaction between the tendencies in the energy, agriculture and waste management sectors.

ACKNOWLEDGMENTS

The present research has been supported by the Latvian National Research Programme 2014–2017 "The Value and Dynamic of Latvia's Ecosystems under Changing Climate (EVIDEnT)".

REFERENCES

1. European Commission. (n.d.). *European Union Climate Strategies & Targets*. Available at http://ec.europa.eu/clima/policies/strategies/index_en.htm
2. Ministry of Economics of the Republic of Latvia. (2016). Informative Report *"Republic of Latvia. Third Report according the Article 22 of the Directive 2009/28/EC of the European Parliament and of the Council of 23 April 2009 on the promotion of the use of energy from renewable sources and amending and subsequently repealing Directives 2001/77/EC and 2003/30/EC"*, 12 January 2016.
3. Central Statistical Bureau of the Republic of Latvia. (n.d.). *Statistics Database ENG02 "Energy Balance"*. Available at http://data.csb.gov.lv/pxweb/en/vide/vide__ikgad__energetika/?tablelist=true&rxid=cdcb978c-22b0-416a-aacc-aa650d3e2ce0
4. Central Statistical Bureau of the Republic of Latvia. (n.d.). *Statistics Database ENG09 "Electrical Capacity and Produced Electricity from Renewables*". Available at http://data.csb.gov.lv/pxweb/en/vide/vide__ikgad__energetika/?tablelist=true&rxid=cdcb978c-22b0-416a-aacc-aa650d3e2ce0
5. *Rural Development Programme for Latvia 2007–2013*.(n.d.). Available at https://circabc.europa.eu/webdav/CircaBC/MARE/steccostclimat/Library/country_information/latvia/RuralDevelopmentPlan_Latvia_2007-13.pdf
6. Ministry of Economics of the Republic of Latvia. (n.d.) *Information regarding mandatory procurement of electricity: Feed-in payments 2015* (*Informācija par izdotajiem lēmumiem par elektroenerģijas obligāto iepirkumu: komersantiem 2015.gadā obligātā iepirkuma ietvaros izmaksātās summas*), in Latvian. Available at https://www.em.gov.lv/lv/nozares_politika/atjaunojama_energija_un_kogeneracija/informacija_par_izdotajiem_lemumiem_par_elektroenergijas_obligato_iepirkumu/
7. Sorda, G., Sunak, Y., and Madlener, R. (2013). An agent-based spatial simulation to evaluate the promotion of electricity from agricultural biogas plants in Germany. *Ecological Economics 89*, 43–60.

8. Central Statistical Bureau of Republic of Latvia, (n.d.). *Statistics Database: LAG015 "Sown area of agriculture crops"*. Available athttp://data.csb.gov.lv/pxweb/en/lauks/lauks__ikgad__03Augk/?tablelist=true&rxid=cdcb978c-22b0-416a-aacc-aa650d3e2ce0
9. Communication from the Commission. (2014). *Guidelines on State aid for environmental protection and energy 2014-2020 (2014/C 200/01*. Official Journal of the European Union, 28.06.2014. Available at http://eur-lex.europa.eu/legal-content/EN/TXT/PDF/?uri=CELEX:52014XC0628(01)&from=EN
10. *Republic of Latvia Cabinet of Ministers Regulations (CMR) No. 262 of 16 March 2010 "Regulations Regarding Electricity Production Using Renewable Energy Resources and the Procedures for the Determination of the Price"*, issued pursuant to the Electricity Market Law. Available at http://likumi.lv/doc.php?id=207458 (see: Tulkojums)
11. *Republic of Latvia CMR No. 221 of 10 March 2009 (with amendments) "Regulations Regarding Electricity Production and Price Determination Upon Production of Electricity in Cogeneration"*, issued pursuant to the Electricity Market Law. Available at http://likumi.lv/doc.php?id=189260 (see: Tulkojums)
12. JSC Latvijas gāze. (n.d.). *Natural gas end-use tariffs.* Available at http://www.lg.lv/uploads/filedir/File/Norekini/Dabasgazes_tarifi_akcizeta_kurinama.pdf
13. JSC Latvijas Gāze. (n.d.) *Forecasts on natural gas tariffs*. Available at http://www.lg.lv/uploads/filedir/File/Jaunumi/Par_tarifiem/Tarifu_prognozes.pdf
14. Saeima (Parliament) of the Republic of Latvia. (n.d.). *Subsidised Electricity Tax Law.* Available at http://likumi.lv/doc.php?id=262304 (see: Tulkojums).
15. Budzianowski, W.M., and Budzianowska, D.A. (2015). Economic analysis of biomethane and bioelectricity generation from biogas using different support schemes and plant configurations. *Energy 88,* 658–666.
16. Appel, F., Ostermeyer-Wiethaup, A., and Balmann, A. (2016) Effects of the German Renewable Energy Act on structural change in agriculture – The case of biogas. *Utilities Policy* (in press), http://dx.doi.org/10.1016/j.jup.2016.02.013
17. Bauer, F., Hulteberg, Ch., Persson T., and Tamm, D. (2013). Biogas upgrading – Review of commercial technologies. Svenskt Gastekniskt Center AB, SGC Rapport 2013:270. Available at http://www.sgc.se/ckfinder/userfiles/files/SGC270.pdf
18. IEA. (2014). *Biomethane: status and factors affecting market development and trade. A joint study by IEA bioenergy task 40 and task 37.*Available at http://www.bioenergytrade.org/downloads/t40-t37-biomethane-2014.pdf
19. Igliński, B., Buczkowski, R., Iglińska, A., Cichosz, M., Piechota, G., and Kujawski, W. (2012). Agricultural biogas plants in Poland: Investment process, economical and environmental aspects, biogas potential. *Renewable and Sustainable Energy Reviews 16*, 4890–4900.
20. Börjesson, M., and Ahlgren, E.O. (2012). A modelling assessment of gas infrastructural options in a regional energy system. *Energy 48*, 212–226.
21. Hahn, H. (2012). *Guideline for financing agricultural biogas projects (IEE Project 'BiogasIN')*. Kassel: Fraunhofer IWES. Available at http://www.biogasin.org/files/pdf/WP3/D.3.5_IWES_EN.pdf
22. *Economic aspects of biogas plants*. (2007). Biogas Regions: Train the Trainers Seminar, presentation, Wolpertshausen, Germany, November 2007. Available athttp://www.biogasregions.org/doc/Train_the_trainers/01.10_economic_aspects.pdf
23. Pelše, M., and Naglis-Liepa, K. (2012). *Enerģētisko augu audzēšanas izmaksu salīdzinājums un digestāta izmantošanas ekonomiskais efekts.* ESF project "Cilvēkresursu piesaiste atjaunojamo enerģijas avotu pētījumiem", presentation, 17 Au-

gust 2012, Vecauce, Latvia. Available at http://ilga.cs.llu.lv/homepg/energija/wp-content/uploads/2012/09/17_08_2012_Pelse_ekonomika.pdf (in Latvian).

24. Angelini, F. (2011). *Economic analysis of gas pipeline projects*. JASPERS, Knowledge Economy, Energy and Waste Division. Available at http://www.jaspersnetwork.org/download/attachments/4948004/Economic_Analysis_of_Gas_Pipeline_Projects_Final.pdf?version=1&modificationDate=1366387572000&api=v2

ENERĢIJAS RAŽOŠNA NO BIOGĀZES: KONKURĒTSPĒJA UN VEICINĀŠANAS INSTRUMENTI LATVIJĀ

G. Klāvs, A. Kundziņa, I. Kudreņickis

K o p s a v i l k u m s

Atjaunojamo enerģijas resursu (AER) izmantošana ir nozīmīgs faktors enerģijas apgādes drošuma paaugstināšanai, vietējās ekonomiskās attīstības veicināšanai un siltumnīcefekta gāzu emisiju samazināšanai, tā panākot trīskāršā ieguvuma efektu. Autori analizē un novērtē divus galvenos veicināšanas instrumentus – investīciju atbalsta (IA) un elektrības obligātā iepirkuma tarifa (OIT) ietekmi, kuri abi tika izmantoti 2010-2014. gadu periodā, lai nodrošinātu mazas jaudas (līdz $2MW_{el}$) lauksaimniecības sektora biogāzes staciju ekonomisko dzīvotspēju. Pētījuma rezultāti, kas iegūti, izmantojot izmaksu novērtējuma modeli, parāda, ka elektrības ražošanas izmaksas biogāzes stacijās aptuveni atbilda minētajā laika periodā eksistējošiem OIT, kurus noteica atbilstošie Ministru Kabineta Noteikumi par elektrības ražošanu, izmantojot AER. Situācija ir radikāli atšķirīga, ja papildus OIT tiek piešķirts arī IA. Proti, analīze parādīja, ka abu šo iepriekš minēto veicinošo instrumentu kombinācijas piemērošanas prakse Latvijā nav bijusi optimāla, jo tā sniedza nesamērīgi augstu atbalstu biogāzes stacijas attīstītājam. Ilgtermiņa perspektīvā šāds pārkompensēts atbalsts sniedz nepareizus signālus attiecībā uz investīcijām jaunajās tehnoloģijās un rada nevienādas konkurences nosacījumus AER elektrības tirgū. Lai nodrošinātu optimālu atbalstu biogāzes ražošanai, ir nepieciešams analizēt tās izmantošanas dažādus veidus. Ar izmaksu novērtējuma modeli autori rakstā analizē divus šos veidus: biogāzes izmantošana elektrības ražošanai uz vietas mazas jaudas biogāzes stacijā un biogāzes bagātināšana līdz biometānam un tā iesūknēšana zema spiediena dabasgāzes tīklā. Veiktais novērtējums parāda, ka biogāzes bagātināšana prasa mazāku publiskā atbalsta apjomu, salīdzinot ar elektrības ražošanu uz vietas, un tādējādi šī alternatīva ir īpaši apspriežama, ņemot vērā pastāvošo infrastruktūru un tehnoloģijas.

15.09.2016.

LATVIAN JOURNAL OF PHYSICS AND TECHNICAL SCIENCES
2016, N 5

DOI: 10.1515/lpts-2016-0036

SOLID STATE PHYSICS

USE OF COMPUTER-GENERATED HOLOGRAMS IN SECURITY HOLOGRAM APPLICATIONS

A. Bulanovs[1], R. Bakanas[2,3]

[1] Innovative Microscopy Centre, Daugavpils University,
1 Parades Str., Daugavpils, LATVIA
[2] Geola Digital UAB, Vilnius, LITHUANIA
[3] Department of Materials Engineering, Kaunas University of Technology,
Kaunas, LITHUANIA
E-mail: bulanov@inbox.lv

The article discusses the use of computer-generated holograms (CGHs) for the application as one of the security features in the relief-phase protective holograms. An improved method of calculating CGHs is presented, based on ray-tracing approach in the case of interference of parallel rays.

Software is developed for the calculation of multilevel phase CGHs and their integration in the application of security holograms. Topology of calculated computer-generated phase holograms was recorded on the photoresist by the optical greyscale lithography. Parameters of the recorded microstructures were investigated with the help of the atomic-force microscopy (AFM) and scanning electron microscopy (SEM) methods. The results of the research have shown highly protective properties of the security elements based on CGH microstructures. In our opinion, a wide use of CGHs is very promising in the structure of complex security holograms for increasing the level of protection against counterfeit.

Keywords: *diffractive optical elements, digital holography, protective holograms.*

1. INTRODUCTION

Relief-phase holograms are widely used in most security applications such as credit cards and passports. They are suitable for the emboss replication process and are easily mass-produced at a low cost. Holograms are applied to documents or products, and the presence of a hologram is intended to be a reliable indication that the document or product is valid. Modern relief-phase holograms contain a wide range of security and visual effects to make them hard to copy or counterfeit. The present article reviews some additional security effects based on the computer-generated ho-

lograms (CGHs) that can be integrated in the structure of protective holograms. It is commonly considered that a CGH is a result of optical recording of the interference field, which was calculated within a diffraction theory with the help of a computer. The receiving topology of CGHs requires a huge amount of calculation and it is a challenge even for modern computers [1]. Therefore, only simple flat objects can be used for calculation to make it in reasonable time. There are several digital technologies suitable for recording of CHG interference images on the photoresist. The most widely spread ones are the interference optical lithography [2], [3] (the so-called "image-matrix" technology) and e-beam lithography [4].

2. THEORETICAL BACKGROUND

Let us consider calculation of a CGH in the case that is most important for practical use, i.e., reconstruction of a hologram image in parallel rays. In this case, with a laser beam falling on the surface of a hologram, the original image is restored in any plane parallel to the hologram surface. The size of the reconstructed image becomes bigger in proportion to the increase of the distance between the observation plane (frosted screen) and the hologram. In practice, it is convenient to use a greyscale bitmap image as an original one. A relative brightness of dots in the reconstructed image, then, is defined as $K_a = \frac{G_a}{255}$, where $G_a = [0..255]$ is a level of the grey colour of the corresponding pixels in the graphic image. Thus, $K_a = 1$ is for white pixels of the bitmap image, to which the dots with maximal brightness in the reconstructed hologram image correspond. $K_a = 0$ is for black pixels of the bitmap image for which there is no correspondence in the hologram (dots with zero brightness).

The aim of the theoretical part of this paper is to demonstrate how a required change in phase for the reflected wave can be calculated for each *B* segment in the hologram (Fig. 1). Given local changes of the reflected wave front, it is easy to calculate the required micro relief topology of the hologram surface. Thus, the maximal depth of the hologram relief $\Delta h = \frac{\lambda}{2}$ corresponds to the change of the phase by $\Delta\varphi = 2\pi$. As far as intermediary values $\Delta\varphi$ are concerned, the relief depth is proportionate to the phase:

$$\Delta h = \frac{\lambda}{4\pi}\Delta\varphi, \tag{1}$$

where λ is length of the wave for which the CGH is calculated.

Let us assume that the original flat image consists of the finite number of dots and is formed in plane ψ (Fig. 1), which is parallel to the hologram surface and is situated at the distance *Z* from it. Let us now find the result of interference of all flat waves passing through active dots of the image to the centre of a CGH.

For one of the image dots, $A = (X_a, Y_a, Z)$ (Fig. 1), this direction is vector $\overrightarrow{OA}$, and plane Ω_a corresponds to the wave front surface passing through the hologram centre *O* (Fig. 1).

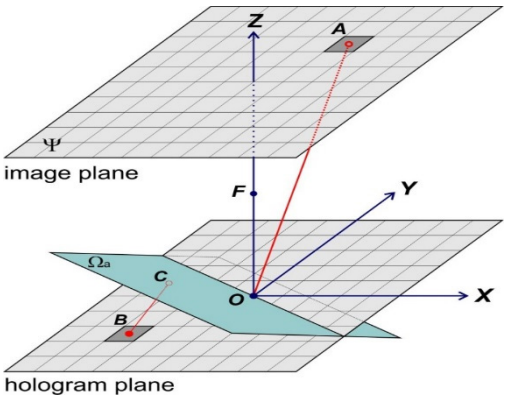

Fig. 1. Sketch for explaining CGH calculation.

Then $\overrightarrow{n_a} = \frac{\overrightarrow{OA}}{|\overrightarrow{OA}|} = \left(\frac{X_a}{L_a}, \frac{Y_a}{L_a}, \frac{Z}{L_a}\right),\ where\ L_a = \sqrt{X_a^2 + Y_a^2 + Z^2}$ will be a unit vector of the normal line to plane Ω_a.

Phase ψ_a of wave front Ω_a has an unspecified arbitrary value in the range [0..2π].

The distance from dot $B = (X_b, Y_b, 0)$ of the hologram to plane Ω_a

$$S_a = BC = \left(\overrightarrow{OB} \cdot \overrightarrow{n_a}\right) = \frac{X_b X_a}{L_a} + \frac{Y_b Y_a}{L_a},\ where\ \overrightarrow{OB} = (X_b, Y_b, 0) \tag{2}$$

Taking into account (2), the phase of flat wave in dot *B* from source *A* is

$$\varphi_a = \frac{2\pi}{\lambda} S_a + \psi_a = \frac{2\pi}{\lambda L_a}(X_b X_a + Y_b Y_a) + \psi_a \tag{3}$$

Complete complex amplitude of interference field in dot *B* is determined by the sum total of complex amplitudes of the object waves from all elemental sources of the original image and reference wave:

$$\dot{A_b} = \sum_a A_0 K_a e^{-i\varphi_a} = A_0 \sum_a K_a e^{-i\varphi_a} \tag{4}$$

Flat wave front that is parallel to the hologram surface was appointed as a reference wave. In (3), the additive component, similar to the one in dot (0, 0, Z) of the image, corresponds to the reference wave. Amplitudes of object waves $A_0 K_a$ are proportional to the brightness of corresponding graphic dots. Formula (4) allows for determining the required change of phase in all dots *B* of the hologram for reconstructing a diffractive image:

$$\varphi_b = \tan^{-1}\left(\frac{Im(\dot{A_b})}{Re(\dot{A_b})}\right) = \tan^{-1}\left(\frac{\sum_a K_a \sin(\varphi_a)}{\sum_a K_a \cos(\varphi_a)}\right), \quad \varphi_b \in [0..2\pi) \tag{5}$$

In case of protective holograms, phase modulation of the reflected wave, in accordance with (5), is defined by the micro relief height of the hologram surface following (1). The image of the CGH object will be reconstructed in the parallel rays; the process can be observed only with the help of a frosted screen or a specially selected lens. For direct observation of the reconstructed object, it is necessary to add the phase function of a lens to the phase surface of the hologram (5). A complete phase of the hologram sector in dot *B* will then be:

$$\phi_b = \varphi_b + \varepsilon_b \text{ , where } \varepsilon_b \text{ is a lens phase function.} \tag{6}$$

Let us find ε_b for a thin lens with the focus in dot F and focal distance *F*=OF (Fig. 1). An optical difference between the travels of beams for a virtual lens in dot *B* will be:

$$\Delta l_b = n\left(\sqrt{F^2 + X_b^2 + Y_b^2} - F\right) \approx n\frac{X_b^2 + Y_b^2}{2F},$$

where $n \approx 1.5$ is a refractive index of the virtual lens material. The phase surface of the flat wave after passing though the virtual lens is:

$$\varepsilon_b = \frac{2\pi}{\lambda}\Delta l_b = \frac{\pi m}{\lambda F}\left(X_b^2 + Y_b^2\right) \tag{7}$$

In (7), value ε_b corresponds to a negative lens, and magnitude $-\varepsilon_b$ indicates a collecting lens. If CGH is calculated following (6), only a remote point light source is necessary for observing of the reconstructed image. A spherical wave from the remote point source of light within the rage of a linear size of CGH can be considered flat with a high degree of precision. Since the calculation of CGH is carried out for a particular wavelength, observation of a CGH with the help of a lamp or the sun will yield a reconstructed image that is blurred and coloured due to spectral selectivity of CGH.

3. EXPERIMENTAL PART

A special computer program was developed for calculating CGHs. For this purpose, an 8-bit greyscale bitmap image was used as a flat object for CGH calculation. The dots of grey scale level define relative brightness of the reconstructed image. The maximal size of the original graphic file is 150x150 pixels. For recording on the photoresist with the resolution of 12500dpi, a discretisation spacing was chosen as d=2um. The maximal diffraction angle with this resolution equals $\alpha = \frac{\lambda}{2d} = 0.15$ for λ=600nm. With these parameters of calculating a CGH, the reconstructed image is approximately 30mm in size at the distance of 100mm from the hologram surface.

The discretisation spacing of the original image was chosen equal to 30/N mm (N is maximal size of the bitmap image in pixels), which corresponded to the

distance of 100mm between the hologram and the plane of observing the image. The results of calculating of a CGH according to (5) and (6) were recorded in a file compatible with the format of the files for the DifX optical lithography device aimed at recording of protective holograms [5], [6]. During the optical recording of a CGH, information about the phase of the current dots is extracted from the file, and the image is calculated for displaying on the SLM and further projection on the photoresist. One cycle of calculating of an image of the size 1920x1080 pixels for the Spatial Light Modulator (SLM) takes about 100 ms. Figure 2 shows part of the image calculated for displaying on the SLM.

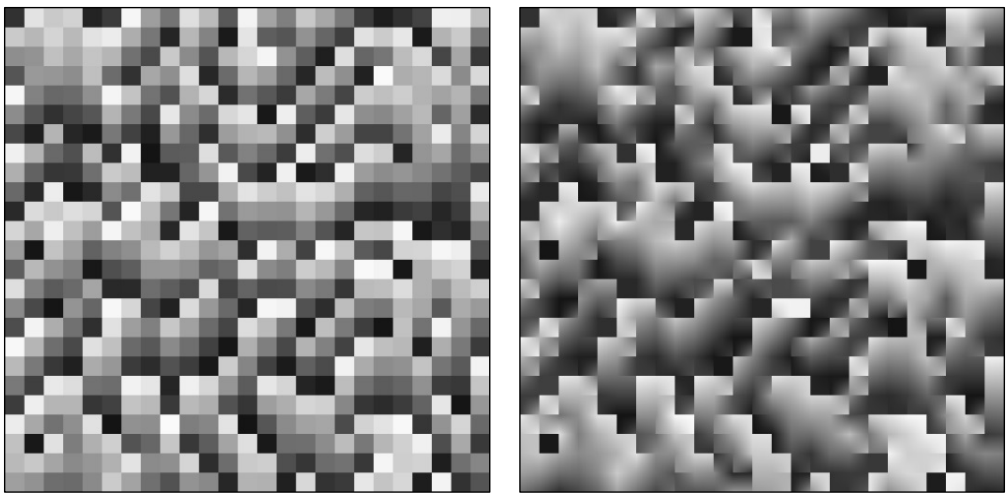

Fig. 2. Part of the CGH bitmap image calculated by the software.
a) Initial image after calculation.
b) Calculated image after approximation procedure.

In Fig. 2a, the program of the optical recording device is getting the image ready for recording of the section of a CGH directly according to the calculation data from the file. In Fig. 2b, an approximation option is used for calculating intermediary values in the framework of every discrete sector of a CGH while preparing the image for displaying on the SLM.

For recording of a CGH on the photoresist, a commercially available system for optical lithography DifX [6] was used. A simplified sketch of the optical scheme for CGH recording is shown in Fig. 3a. *S*-polarized laser beam **1** is directed by the polarising beam splitter **3** on the LCOS [7] (Liquid Crystal on Silicon) modulator **2**. When there is no signal (black coloured pixels), the polarization plane of the light reflected from the LCOS SLM does not change, and the laser beam is directed by the beam splitter **3** in the initial direction **1**. When the colour of pixels changes, the polarization plane of the light reflected from the SLM turns, and part of the radiation with *P*-polarization passes through the beam splitter **3** in the direction of focusing optics **4** and is projected on the photoresist **5**.

An important precondition of recording of qualitative relief-phase CGHs is a precise linear and proportional correspondence between the level of the grey colour in the image calculated for the SLM and the corresponding depth of the relief on the photoresist.

At the first stage of preparation to recording, a linear working range of the LCOS modulator was determined. A calibration schedule of the dependence of laser radiation intensity in the photoresist plane on the level of the grey colour of the image (Fig. 3b) was obtained experimentally. In course of experiment, an evenly coloured image with 8-bit greyscale value in the range [0..255] was displayed on the modulator. For each grey colour value, intensity of radiation in the recording place was measured. Figure 3b shows a calibration scale for LCOS SLM, with the use of the manufactured tuning controls.

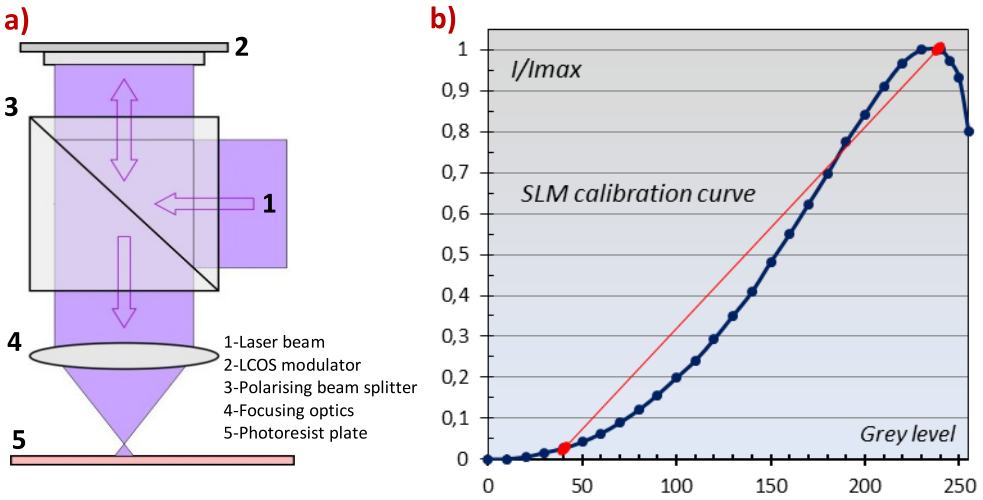

Fig. 3. a) Sketch of the optical scheme for CGH recording.
b) Calibration curve for multilevel CGH recording.

It is worth mentioning that a calibration curve may be adjusted with the help of parameter controls of the modulator drivers. In our case, though, this was not done because of the influence of the changed controls on other work modes of the optical lithography device.

A greyscale range of 40–230 was selected as a linear working range for optical recording (red line, Fig. 3b). The linear interdependence between the grey colour level and exposition is satisfactorily realised in this selected range. At the second stage of the adjustment of optical recording, an optimal exposition was determined; with it, the depth of the relief on the photoresist corresponded to the calculated value (1). For this purpose, an image of lines coloured with the gradient of the grey colour change (Fig. 4a) was projected on the photoresist from the modulator.

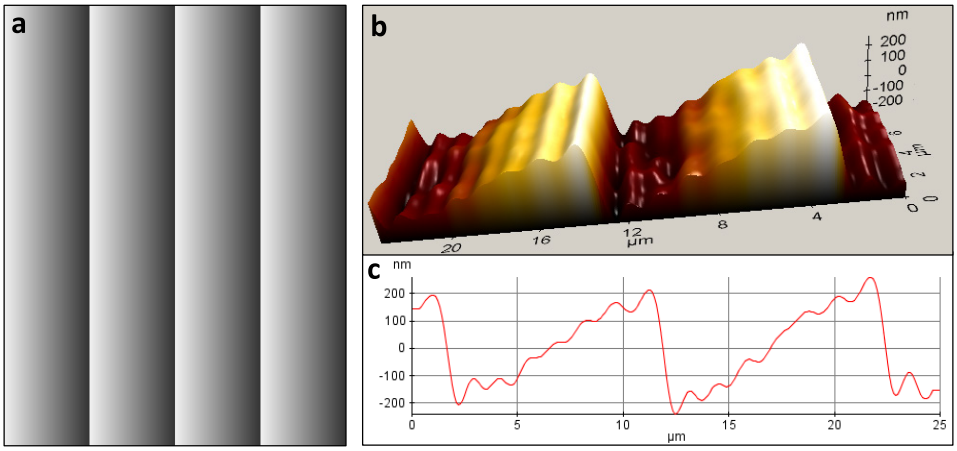

Fig. 4. a) Part of calibrated image for sawtooth grating recording.
b) AFM image of recorded sawtooth grating.
c) Profile of recorded sawtooth grating.

The range of colour change corresponded to a linear segment of the SLM calibration curve. The width of the lines after projection on the photoresist was 10um, a test exposure dose was 20mJ/cm^2. We used the photoresist AZ1514H [8] for recording; it was deposited on the glass substrate of the size 5x5 inch by the spin coating method. The photoresist layer was about 2um thick. Development of the exposed plates was performed by the water solution of the concentrate AZ303 in the 1:4 proportions during 10 sec at 20^o C. A linear dependence of the development speed on exposition was expected. An AFM (Park Systems NX10) was used to analyse relief and profile of the obtained diffraction gratings. On the basis of the obtained data (Fig. 4b, c), an optimal exposition 12mJ/cm^2 was chosen for recording of a CGH with the 300nm relief depth. Using optimal parameters of optical recording, test samples of CGH calculated using (5) and (6) were produced.

4. RESULTS AND DISCUSSION

A bitmap image of size 100x100 dots was used to calculate CGHs. Approximate calculation time of CGH of 5000x5000 pixels was 5 min for the “hidden image” effect [9] (Fig. 4a, b) and around 15 min for the “image in lens” effect (Fig. 4c). With the discretisation spacing equal to 2um, the size of CGH of 5000x5000 pixels was 1 cm^2 (10x10 mm) on the photoresist; optical recording of samples took around 30 min (recording speed was about 2cm^2/hour). After recording and development procedures, surface topology of the samples was investigated with the help of scanning electron microscopy (SEM). Figure 3a shows a surface segment of 80x80um of a relief-phase digital hologram. This segment contains 40x40=1600 calculated pixels. Figure 3b presents an AFM image of a part of the same hologram, showing that the relief height of the hologram surface remains within the required calculated range of 0–300um.

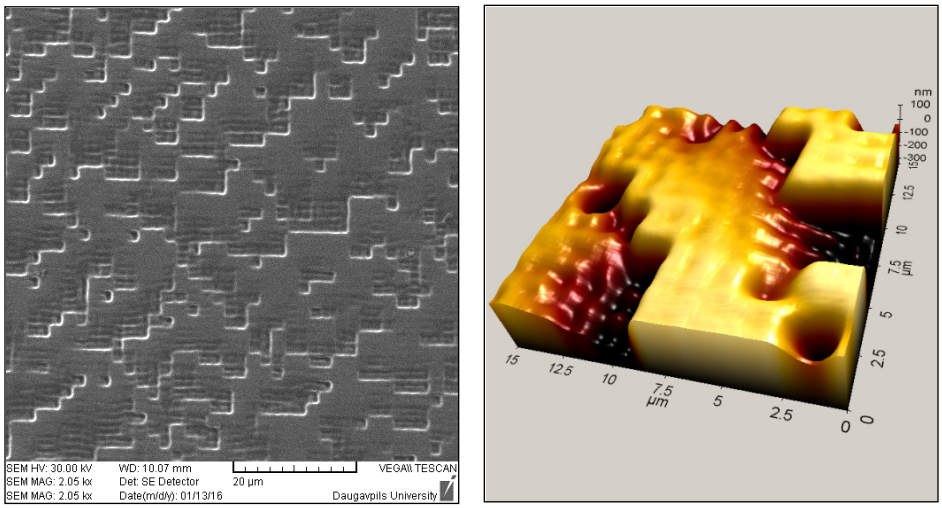

Fig. 3. a) SEM image of photoresist surface with a CGH element.
b) AFM image of photoresist surface with a CGH element.

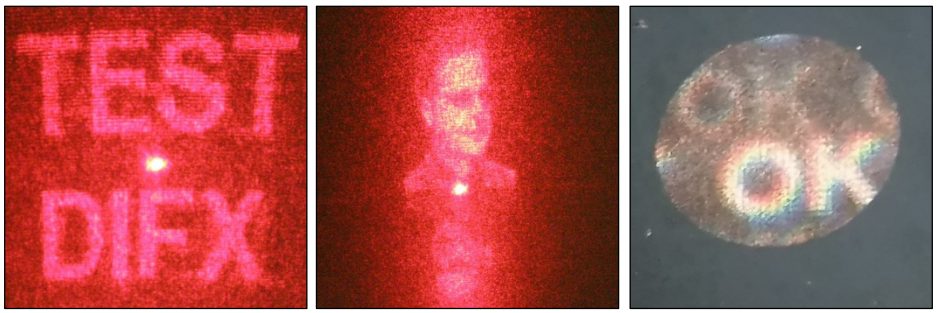

Fig. 4. a), b) Photos of the image recovered from the "hidden image" CGH on a scattering screen.
c) Photo of the photoresist surface with the "text in lens" CGH element.

Figure 4a, b demonstrates photos of the image recovered from a "hidden image" CGH on a scattering screen. A photo of the photoresist surface with the "text in lens" CGH element, which was made under a point like light source, is shown in Fig. 4c. After optical recording and development, CGH samples were coated with a ~10-15nm layer of silver with the help of a vacuum deposition method (reflection about 95 %). The reconstructed image was formed by a laser beam reflected from the CGH surface on the scattering flat screen. For diffraction efficiency (DE) evaluation of CGH samples, the following formula was used:

$$DE = 100\% \cdot \frac{I_0 - I}{I_0}, \tag{8}$$

where I_0 is intensity of the laser beam falling on a CGH, and I is intensity of the zero order diffraction in the reflected beam. The measured DE in the obtained samples of CGH was within the range of 80–85 %. A semiconductor laser, with the power P=5mW and the wavelength λ=630nm, was used to perform the measure-

ments. Taking into account unwanted diffraction and scattering effects, the real DE corresponding to the useful image was evaluated in the range of 70–75 %. A high DE allowed for realising the so-called "asymmetric hidden image" security effect (Fig. 4a). Considerable inhibition of symmetric mirror images for the I_{+1} and I_{-1} order diffraction helped place various original images in these diffraction orders avoiding overlapping. Formula (5) contains coefficients related to the relative brightness of dots in the original image to calculate CGHs. This option allows using a greyscale photo or image to calculate a hologram (Fig. 4b). An "asymmetric hidden image" (Fig. 4a) is one of the most complicated features of counterfeit, and checking it always requires a laser pointer and scattering screen, which is not convenient in some cases. The security effect calculated by (6) adds to the CGH phase function of the virtual spherical lens and makes the recovered image visible like through a real lens. Visually, this effect is very impressive and can be observed in the sunlight or other point light sources.

5. CONCLUSION

The present paper is devoted to the calculation and study of CGH recording parameters in the situation of their use in a complex structure of relief-phase protected holograms. A complex mathematical calculation and strict requirements for the parameters of optical recording make CGH elements difficult to counterfeit. The software for CGH calculation was created on the basis of the proposed improved ray-tracing algorithm. The created software for calculating of CGHs is completely compatible with the DifX system of recording of protective holograms and allows using CGHs of any shapes and sizes in the complex structure of a protective hologram. It should be noted that the number of visual and security effects implemented using CGH can be potentially greater than described. For example, protective effects to form an image in only certain predefined planes can be achieved, which might be useful in automatic authentication of security holograms.

ACKNOWLEDGMENTS

The present research has been partly supported by the National Research Programme of Latvia "Multifunctional Materials and Composites, Photonics and Nanotechnology (IMIS2)".

REFERENCES

1. Murano, K., Shimobaba, T., Sugiyama, A., Takada, N., Kakue, T., Oikawa, M., and Ito, T. (2014). Fast computation of computer-generated holograms using Xeon Phi coprocessor. *Computer Physics Communications, 185 (10)*, 2742–2757, DOI: 10.1016/j.cpc.2014.06.010.
2. Bulanovs, A., Tamanis, E., and Mihailova, I. (2011). Holographic recording device based on LCoS spatial light modulator. *Latvian Journal of Phys. and Tech. Sciences*, *48 (5)*, 60–68, DOI: 10.2478/v10047-011-0034-5.

3. Bulanovs, A., Gerbreders, V., Kirilovs, G., and Teteris, J. (2011). Investigations of As-S-Se thin films for use as inorganic photoresist for digital image-matrix holography. *Central European Journal of Physics*, DOI: 10.2478/s11534-010-0133-6.
4. Firsov, An., Firsov, A., Loechel, B., Erko, A., Svintsov, A., and Zaitsev, S. (2014). Fabrication of digital rainbow holograms and 3-D imaging using SEM based e-beam lithography. *Optics Express, 22 (23)*, 28756–28770, DOI: 10. 1364/0E. 22. 028756.
5. Bulanovs, A., and Gerbreders, S. (2013). Advanced concept for creation of security holograms. *Latvian Journal of Phys. and Tech. Sciences, 50 (6),* 61–70, DOI: 10.2478/lpts-2013-0041.
6. InnoSol. (n.d.). Retrieved 17 April 2016, from www.difx-holo.com
7. Holoeye. (n. d.). Retrieved 17 April 2016, from www.holoeye.com
8. MicroChemicals. (n.d.). Retrieved 17 April 2016, from www.microchemicals.com
9. Bulanovs, A., Tamanis, E., and Kolbjonoks, V. (2013). The 'hidden image' effect in security holograms and its personalization by laser demetallization. *Proc. SPIE 8776, Holography: Advances and Modern Trends III,* 87760R, DOI:10.1117/12.2017135.

DATORA ĢENERĒJOŠO HOLOGRAMMU IZMANTOŠANA DROŠĪBAS HOLOGRAMMU PIELIKUMOS.

A. Bulanovs, R. Bakanas

K o p s a v i l k u m s

Rakstā ir apskatīta datora ģenerējošo hologrammu izmantošana kā vienu no drošības pazīmēm reljefa-fāzes aizsardzības hologrammām. Parādīta datora ģenerējošo hologrammu aprēķina uzlabota metode, paralēlo staru interferences gadījumā. Izstrādāts programmnodrošinājums datora ģenerējošo hologrammu daudzlīmeņu fāzes aprēķinam, un to integrācija drošības hologrammu struktūrā. Aprēķinātās fāzes hologrammas mikrostruktūra tika ierakstīta uz fotorezista ar optiskās litogrāfijas palīdzību. Ierakstīto mikrostruktūru parametri tika pētīti ar atomu-spēka mikroskopijas un skenējošas elektroniskās mikroskopijas metožu palīdzību. Darba rezultāti parādīja datora ģenerējošo holografisko elementu mikrostruktūru augstas drošības īpašības. Mūsuprāt, datora ģenerējošo holografisko elementu plaša izmantošana sarežģīto drošības hologrammu struktūrā ir perspektīva, jo ļauj palielināt aizsardzības līmeni pret viltošanu.

16.05.2016.

LATVIAN JOURNAL OF PHYSICS AND TECHNICAL SCIENCES
2016, N 5

DOI: 10.1515/lpts-2016-0037

ELECTRONICS

INVESTIGATION OF SERVICE QUALITY OF MEASUREMENT REFERENCE POINTS FOR THE INTERNET SERVICES ON MOBILE NETWORKS

E. Lipenbergs, Vj. Bobrovs, G. Ivanovs

Department of Telecommunications, Riga Technical University
12 Azenes Str., Riga, LV-1010, LATVIA
e-mail: elmars.lipenbergs@rtu.lv

To ensure that end-users and consumers have access to comprehensive, comparable and user-friendly information regarding the Internet access service quality, it is necessary to implement and regularly renew a set of legislative regulatory acts and to provide monitoring of the quality of Internet access services regarding the current European Regulatory Framework. The actual situation regarding the quality of service monitoring solutions in different European countries depends on national regulatory initiatives and public awareness. The service monitoring solutions are implemented using different measurement methodologies and tools. The paper investigates the practical implementations for developing a harmonising approach to quality monitoring in order to obtain objective information on the quality of Internet access services on mobile networks.

Keywords*: Internet access, quality of service.*

1. INTRODUCTION

The electronic communications sector is characterised by the dynamic development of broadband electronic communications networks in mobile environment.

To maintain a high quality level by the dynamic variations of technologies for provided services, the national regulatory authority should carefully follow all aspects of regulated service quality in the electronic communications sector, determine service quality parameters, their values and perform measurements to ascertain if quality requirements imposed for electronic communications services are complied with.

The scope of investigations included in this paper also covers the topics defined under the Position documents and Regulation of the European Parliament and of the Council, which entered into force last quarter of 2015.

Furthermore, the consumers require the explanation of the minimum, actual, normally available, maximum and advertised download and upload speed of the Internet access services, particularly for mobile Internet services.

The main objective of the research is to compare different measurement approaches in order to find the optimal solution for the quality assessment of Internet access services on mobile networks. The paper includes the recommended quality parameters and reference points of the mobile Internet access services from the consumer perspective. Certain types of mobile broadband measurements are provided practically using measurement initialising software on notebook computer and Visualware Inc [1] measurement system software placed on server connected to the Internet exchange point. Application of Quality of Service (QoS) measurement metrics considered in the paper is useful as the basis for further research.

2. LEGISLATIVE ACTS AND REGULATORY FRAMEWORK

The Internet has developed over the past decades as an open platform for innovation with low access barriers for end-users, providers of content, applications and services and providers of Internet access services. The existing regulatory framework aims to promote the ability of end-users to access and distribute information or run applications and services of their choice [2].

To reach main goals concerning open Internet access, the European Parliament and the Council of 25 November 2015 are laying down measures concerning open Internet access and amending Directive 2002/22/EC on universal service "Universal Service Directive" and users' rights relating to electronic communications networks and services and Regulation (EU) No 531/2012 on roaming on public mobile communications networks within the Union [2]. The Position (EU) No 14/2015 of the Council at the first reading with a view to the adoption of a Regulation concerning open Internet access was adopted by the Council on 1 October 2015 [3].

Article 22.1 of the Universal Service Directive (USD) requires the Member States to ensure that undertakings providing publicly available electronic communications services publish comparable, adequate information for end-users on the quality of their services. At the same time, USD 22.2 encourages regulatory bodies to specify, inter alia, the quality of service parameters to be measured and the content, form and manner of the information to be published in order to ensure that end-users have access to comprehensive, comparable, reliable and user-friendly information [4].

To provide information on the best practices for monitoring the quality of retail Internet access services and recommend a harmonized minimum set of parameters and measurement methods, there are the following technical documents – The European Conference of Postal and Telecommunications Administrations (CEPT) Electronic Communications Committee Report 195 (ECC Report 195) on Minimum Set of Quality of Service Parameters and Measurement Methods for Retail Internet Access Services [5], and CEPT ECC Recommendation (15)03 (ECC Recommendation 15) on Provision of Comparable Information on Retail Internet Access Service Quality [6].

Degradation of network performance of IP-based networks may be due to general congestion in the network or targeted traffic management may cause it. Descriptions of these issues are included in the Body of European Regulators for Electronic Communications (BEREC) documents related to the framework for quality of service in the scope of net neutrality [7]–[9].

European Telecommunications Standards Institute (ETSI) and International Telecommunication Union (ITU) deliverables, namely ETSI EG 202 057 [10], ETSI TS 102 250 [11], ETSI EG 203 165 [12], ETSI EG 202 765 [13], ITU-T Recommendations Y.1540 [14] and Y.1541 [15], establish and define a set of user related QoS parameters.

3. OVERVIEW OF BASIC MEASUREMENT PRINCIPLES

What parameters should be measured, how they should be measured and where they should be measured – these are essential questions for receiving comparable information on the quality of Internet Access Services. Parameters about transmission speed, delay, delay variation, packet loss ratio and packet error ratio are necessary for evaluating the quality of retail Internet access services. Classification of measurement principles by QoS assessment reference points is possible by the following scenarios [5]:

A. QoS Evaluation of the Internet Service Provider Leg

Only the network section directly influenced by the Internet service provider will be assessed. The Internet service provider leg consists of the access network part and the service provider network part of the connection of the customer to the Internet service provider [10].

B. QoS Evaluation of the Access to National Internet Exchange Point

By the QoS evaluation of the access to a national internet exchange point (IXP), the test server is located at a national IXP. This scenario will allow comparing the QoS access to the IXP of the different Internet service providers in a specific country.

C. QoS Evaluation of Access to International IXP

For the QoS evaluation of the access to an international IXP the test servers are located at national internet exchange points in several countries. This would allow for comparisons between the connectivity of Internet access services of different countries. This test scenario practically covers the QoS assessment for international links with different countries.

4. RELEVANT PARAMETERS FOR INTERNET ACCESS QOS ASSESSMENT

Based on the analysis provided in ECC Report 195 and ECC Recommendation 15, it may be concluded that five groups of parameters are relevant for inclusion in the minimum set for the general evaluation of the Internet access services [5], [6].

A. Transmission Speed

Transmission speed minimum and average values are expressed in megabits per second (mbps) or kilobits per second (kbps). The data transmission rate is achieved separately for downloading and uploading of specified test files between a remote web site and a user's terminal equipment – computer [5], [10].

B. Delay

Delay average value is expressed in milliseconds (ms). The delay is half the time in milliseconds that is needed for an Internet Control Message Protocol (ICMP) Echo Request/Reply (Ping) to a valid IP address [5], [10]. Some measurement tools provide the Round-Trip Time (RTT) assessment that is the length of time it takes for a signal to be sent plus the length of time it takes for a signal to be received.

C. Delay Variation

Delay variation or Jitter value is expressed in milliseconds (ms). For a given pair of IP packets, parameters represent the difference between the delays in one direction measured for two consecutive packets [5], [14]–[15].

D. Packet Loss Ratio

Packet loss ratio value is expressed in percent (%). It is the ratio of total lost IP packet outcomes to total transmitted IP packets in a population of interest [5], [14].

E. Packet Error Ratio

Packet error ratio value is expressed in percent (%). It is the ratio of total errored IP packet outcomes to the total of successful IP packet transfer outcomes plus errored IP packet outcomes in a population of interest [5], [14].

5. QoS MEASUREMENT TECHNIQUES USED FOR THE EXPERIMENTS

Before the profound investigation, the QoS measurements were performed as a feasibility study to various reference points with different measurement tools located in different places within the Internet environment. Usually the test servers are hosted by Internet service providers and connected to their core network nodes. The access capabilities to the operator test servers differ from other Internet access service providers because the interconnection links are sometimes of very different capacity. More equivalent measurement results are achieved when the dedicated test

server and reference point are located abroad but this way allows assessing the international links without objective possibility to compare Internet service providers at a national level. The achieved measurement results, particularly on mobile networks, sometimes are obtained incomparable because the measurement techniques and algorithms were different. These obstacles require some unified approach to apply for the provided measurements.

For the investigations, measurements were performed by lots of web interface based online tools, more focused on OOKLA Speedtest tool [20], RTR-NetTest online tool [21], Visualware Inc. online test tool [1] and Latvian regulatory authority – SPRK Internet access QoS measurement system ITEST [16].

OOKLA Speedtest tool ranks mobile networks using the average download performance for the fastest available technology. This provides an accurate view of the typical performance you can achieve using a modern smartphone or tablet on a given mobile network [21].

RTR-NetTest online tool allows measuring speed of data connection in both directions – downlink/uplink and latency of data connection. RTR-NetTest online tool is located at Austrian national internet exchange point and this test tool practically covers the QoS assessment for international links from different countries.

Visualware Inc. online test tool provides different types of Internet access tests such as speed measurements, VoIP measurements, quality and video streaming tests. Visualware Inc. measurement tool uses reference servers located in different countries around the world and this test tool also covers the QoS assessment for international links.

Comparing different options of measurement principles classified by QoS assessment reference points and measurement software types, further investigations are provided via the user interface of web page based measurement software. The measurement server is located nearby the Internet exchange point and with 1-Gibabit links is connected to the main exchange point.

General measurement principles and connection data flows are shown in Fig. 1.

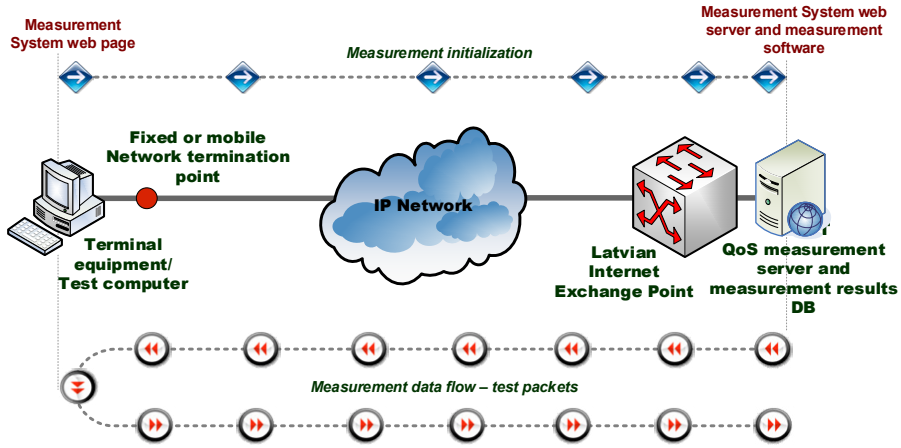

Fig. 1. Illustration of QoS measurement reference points and general QoS evaluation principles with access to a national internet exchange point [5].

As measurement system software Visualware Inc. [1] module "MyConnection Server BusinessCenter" was used. The Internet access QoS measurement system IT-EST is hosted by the Latvian regulatory authority – SPRK and is freely accessible at SPRK's website [16] from Latvian IP addressing space. The measurements were performed on three mobile GSM/UMTS operator's networks using notebooks with Windows operating system (Internet Explorer and Chrome browsers) with sequentially connected Huawei USB stick modems E3372 and Huawei E593 type routers, which support communication in all typical frequency ranges for 3G and 4G services [17], [18], [19].

Two types of measurements were performed in this paper – short-term measurements in different geographical locations and long-term measurements in certain locations. As the routers were collocated quite closely, for the most sure and believable measurement results the USB dongles and routers were connected one by one to exclude simultaneous data transmission and to avoid possible radiofrequency signal interference. The used measurement sequence scenarios defined by measurement management software script commands and for one measurement cycle are shown in Fig. 2. In the first scenario, three measurement sessions are provided in one operator's network. The second scenario allows changing the operator's networks for each new measurement session. The advantage of this scenario is better measurement sequence but this scenario requires the extra time for equipment reconnecting to the networks after a single measurement session.

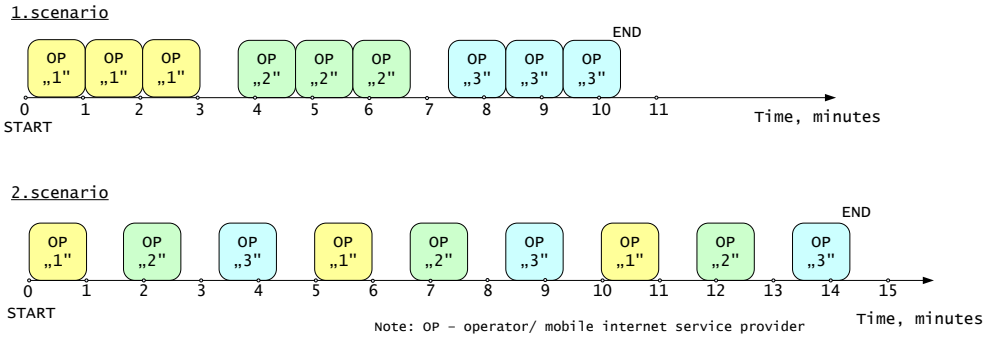

Fig. 2. QoS measurement session sequence scenarios.

6. PROCESSING OF QOS MEASUREMENT RESULTS

The main objective of this section of the paper is to compare two types of provided measurements in order to make conclusions in a given area from the consumer perspective.

For the short-term measurements, average values gathered during all measurement sessions were produced and calculated as arithmetic mean values categorized by network technology by each measurement location and as common value per operator's network. For the long-term measurements, transmission speed average values were processed within one-week and one-day frame calculating arithme-

tic mean values hour by hour. One-day example of the long-term measurements is shown in Fig. 3.

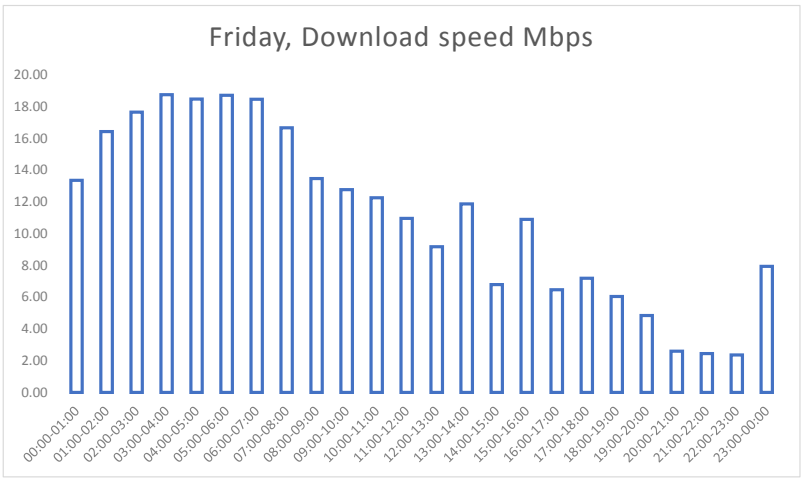

Fig. 3. Example of the long-term measurements of 4G download speed value deviation during 24 hours.

Collected measurement data were processed for the download and upload transmission speed, latency, delay variation or jitter and packet loss ratio. The latency deviation was about 300 milliseconds on 2G networks, about 60 milliseconds on 3G networks and up to 30 milliseconds on 4G mobile networks. For instance, recommendation is that one-way latency should not exceed 150 milliseconds. The collected measurement data were divided by generations of mobile technologies for calculating average latency variations on mobile networks. As shown in Fig. 4, latency value on 4G mobile networks is quite enough to ensure comfortable use of all services available on the Internet if the Internet access speed is sufficient for providing specific services.

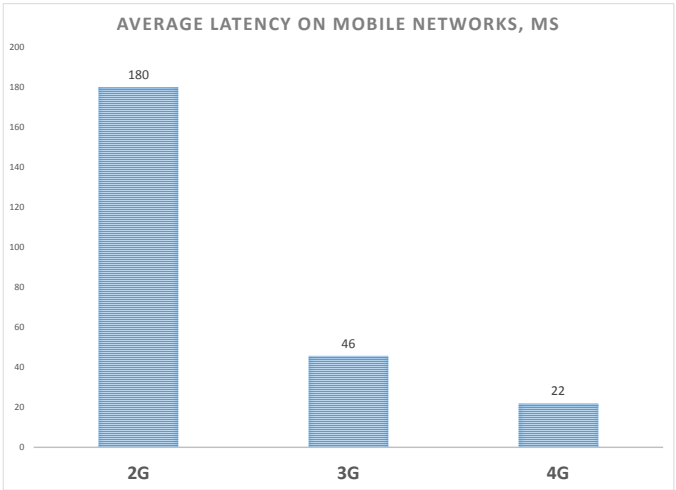

Fig. 4. Example of the average round-trip latency variations for different generations on mobile networks.

The actual measured transmission speed maximum values depend on 3G or 4G network technologies provided in a given measurement location. Typically, maximum actual transmission speed by dedicated previously mentioned measurement conditions does not exceed 30 % of maximum theoretical speed advertised by vendors – 100 or 150 Mbps, while the deviation of the transmission speed strongly depends on the Internet usage activities in a certain geographical area.

7. CONCLUSIONS

The proposed measurement techniques applying the same measurement tool to all measurements and using dedicated reference points, i.e. from a network termination point to a national Internet exchange point, allow reaching reliable and comparable information about mobile broadband Internet access quality provided to consumers. The provided measurement methodology offers the guidance for the practical implementation of regulatory framework regarding comprehensive and user-friendly information publishing.

Taking into account that the mobile network performance in peak hours and by "heavy" user's activities slows down, short-term measurements are more useful if a large number of measurement places are chosen. However, long-term measurements give the objective information about the Internet service capability available to end-users and network resources sufficiently during a daytime.

REFERENCES

1. Visualware Inc. Available at http://www.visualware.com/
2. Regulation (EU) 2015/2120 of the European Parliament and of the Council of 25 November 2015 laying down measures concerning open internet access and amending Directive 2002/22/EC on universal service and users' rights relating to electronic communications networks and services and Regulation (EU) No 531/2012 on roaming on public mobile communications networks within the Union.
3. Position (EU) No 14/2015 of the Council at first reading with a view to the adoption of a Regulation of the European Parliament and of the Council laying down measures concerning open internet access and amending Directive 2002/22/EC of the European Parliament and of the Council on universal service and users' rights relating to electronic communications networks and services and Regulation (EU) No 531/2012 of the European Parliament and of the Council on roaming on public mobile communications networks within the Union Adopted by the Council on 1 October 2015.
4. Directive 2002/22/EC of the European Parliament and of the Council of 7 March 2002 on universal service and users' rights relating to electronic communications networks and services (Universal Service Directive).
5. The European Conference of Postal and Telecommunications Administrations (CEPT) Electronic Communications Committee (ECC) Report 195 Minimum Set of Quality of Service Parameters and Measurement Methods for Retail Internet Access Services, 2013.
6. The European Conference of Postal and Telecommunications Administrations (CEPT) Electronic Communications Committee (ECC) Recommendation (15)03: Provision of Comparable Information on Retail Internet Access Service Quality, 2015.

7. The Body of European Regulators for Electronic Communications (BEREC), A framework for quality of service in the scope of net neutrality, Document No. BoR (11) 53, 2011.
8. The Body of European Regulators for Electronic Communications (BEREC), Guidelines for quality of service in the scope of net neutrality, Document No BoR (12) 131, 2012, pp. 8–17, pp. 37–38.
9. The Body of European Regulators for Electronic Communications (BEREC), Report on monitoring quality of Internet access services in the context of net neutrality, Document No BoR (14) 117 2014.
10. ETSI EG 202 057-4 Speech Processing, Transmission and Quality Aspects (STQ); User related QoS parameter definitions and measurements; Part 4: Internet access.
11. ETSI TS 102 250 Speech and multimedia Transmission Quality (STQ); QoS aspects for popular services in mobile networks; Part 1: Assessment of Quality of Service.
12. ETSI EG 203 165 Speech and multimedia Transmission Quality (STQ); Throughput Measurement Guidelines.
13. ETSI EG 202 765 Speech and multimedia Transmission Quality (STQ); QoS and network performance metrics and measurement methods; Part 3: Network performance metrics and measurement methods in IP networks.
14. ITU-T Recommendation Y.1540 Internet protocol aspects – Quality of service and network performance; Internet protocol data communication service – IP packet transfer and availability performance parameters.
15. ITU-T Recommendation Y.1541 (12/11) Internet protocol aspects – Quality of service and network performance; Network performance objectives for IP-based services.
16. Latvian regulatory authority "SPRK". Available at http://www.sprk.gov.lv/.
17. Ancans, G., Bobrovs, V. and Ivanovs, G. (2013). Spectrum usage in mobile broadband communication systems. *Latvian Journal of Physics and Technical Sciences, 50 (3)*, 49–58, DOI:10.2478/lpts-2013-0019.
18. Gessner, C. (2011). Long term evolution: A concise introduction to LTE and its measurement requirements, pp.78–146.
19. Lloyd-Evans, R. (2002). QoS in integrated 3G networks, pp. 64–68, 221–245.
20. Ookla. Available at http://www.ookla.com/
21. Speedtest. Available at http://www.speedtest.net/
22. RTR-NetTest. Available at https://www.netztest.at/

PAKALPOJUMU KVALITĀTES MĒRĪJUMU ATSKAITES PUNKTU PĒTĪŠANA INTERNETA PAKALPOJUMAM MOBILAJOS TĪKLOS

E. Lipenbergs, Vj. Bobrovs, Ģ. Ivanovs

K o p s a v i l k u m s

Lai nodrošinātu lietotājiem pieejamu atjauninātu un atbilstīgu informāciju par interneta piekļuves pakalpojumu kvalitāti, ir jānodrošina pastāvīga regulējošo normatīvo aktu, kā arī pakalpojumu kvalitātes uzraudzībā izmantoto mērīšanas un monitoringa metodiku aktualizācija atbilstoši Eiropas elektronisko sakaru nozares

regulēšanas ietvarā noteiktajām vadlīnijām. Šobrīd, saistībā ar pakalpojumu kvalitātes tehnisko uzraudzību, Eiropas Savienības dalībvalstīs nav ieviesti vienoti mērīšanas instrumenti vai rīki pakalpojumu interneta piekļuves pakalpojuma kvalitātes monitoringa nodrošināšanai, kā arī nav piemērotas vienotas metodikas mērījumu nodrošināšanai. Pakalpojumu kvalitātes uzraudzības praktiskā nodrošināšana katrā Eiropas Savienības dalībvalstī ir atkarīga no nacionālo regulatoru iniciatīvas un tehniskajām iespējām.

Pētījuma nozīmīgākais uzdevums ir pakalpojumu kvalitātes mērīšanas metodikas galveno pamatprincipu definēšana, vienotas un objektīvas kvalitātes uzraudzības nodrošināšanai, tādejādi sniedzot iespējami visaptverošu un salīdzināmu informāciju par pakalpojumu kvalitāti, tās izmaiņām un attīstības tendencēm gan lietotājiem, gan pakalpojumu sniedzējiem. Analizēta dažādu interneta piekļuves pakalpojuma mērīšanai izmantotu algoritmu un mērījumu atskaites punktu jeb mērīšanā ietverto elektronisko sakaru tīklu posmu izmantošana, kā arī nozīmīgāko raksturojošo parametru izvēle kvalitātes novērtēšanā.

Pētījuma rezultātā ir sniegti ieteikumi pakalpojumu kvalitātes uzraudzībā izmantojamo mērīšanas principu piemērošanā, kā vienu no kritērijiem nosakot, ka pakalpojumu kvalitātes mērījumu veicami posmā no elektronisko sakaru tīkla pieslēguma punkta līdz nacionālajam interneta apmaiņas punktam. Tas nodrošina pakalpojumu sniedzējiem iespējami labāko savstarpēji salīdzināmas informācijas iegūšanu, vienlaikus objektīvi raksturojot lietotājiem pieejamo interneta piekļuves pakalpojuma kvalitāti, kā arī pakalpojumu kvalitātes izmaiņu dinamiku.

11.02.2016

LATVIAN JOURNAL OF PHYSICS AND TECHNICAL SCIENCES
2016, N 5

ĪSAIS ZIŅOJUMS

BALTIC FLOWS – JAUNĀKO SASNIEGUMU IZMANTOŠANA LIETUS ŪDENS UZRAUDZĪBĀ UN VADĪBĀ

A.Kalnačs

Fizikālās enerģētikas institūts
Aizkraukles iela 21, Rīga, LV-1006, LATVIJA

Projektu Baltic Flows finansē Eiropas Savienības 7. ietvarprogramma, un tas attiecas uz lietus ūdens uzraudzību un vadību. Projekta uzmanības centrā ir upes un pilsētas Baltijas jūras sateces baseinā, bet ne Baltijas jūra. Projektā, ar mērķi sasniegt jaunu līmeni lietus ūdens uzraudzībā un vadībā, ir apvienotas 17 organizācijas – projekta partneri. Bez šīm organizācijām projektā iesaistījušās arī citas, kopumā 43 organizācijas. Projektā iesaistījušies piecu Baltijas jūras reģiona valstu – Zviedrijas, Somijas, Igaunijas, Latvijas un Vācijas pārstāvji, viens projekta partneris no Lielbritānijas, kas specializējies Ķīnas vides sektorā, kā arī 30 organizācijas, kas atbalsta projektu, ieskaitot institūcijas Eiropas reģionos un partneru organizācijas no dažādiem pasaules reģioniem: Baltkrievijas, Krievijas, Ķīnas, Vjetnamas un Brazīlijas.

Latviju projekta konsorcijā pārstāv trīs organizācijas:

- Fizikālās Enerģētikas institūts,
- Latvijas vides investīciju fonds,
- Rīgas plānošanas reģions

Lietus ūdens lielos daudzumos veido strautus un upes. Pilsētvidē stipras lietusgāzes rada plūdus. Gadu gaitā lielākā daļa no šī lietus ūdens nonāk jūrā. Ziemeļeiropā šo ilggadīgo lietus ūdens vēsturi uzkrāj Baltijas jūra. Līdz ar to ūdens kvalitāte tajā lielā mērā ir atkarīga no Baltijas jūras valstu īstenotās politikas piesārņojuma un ūdens kvalitātes jomā.

Projekts Baltic Flows balstās uz ideju, ka lietus ūdens ir jāuzrauga un jāvada, pirms tas sasniedz jūru. Piesārņojums ir jākonstatē pēc iespējas ātrāk – vistuvāk vietām, kur tas rodas – labāk jau upju augštecēs, nekā lejteču reģionos. Lai to panāktu, iespējams izmantot trīs tendences, kas mūsdienu sabiedrībā arvien pastiprinās:

- tehnoloģisko risinājumu miniaturizācija,
- arvien aktīvāka iedzīvotāju iesaistīšanās dažādu problēmu risināšanā ar sociālo tīklu palīdzību,
- izpratnes par pilsētvides plānošanu palielināšanās.

Minēto tendenču pastiprināšanos apliecina arī projekta Baltic Flows ietvaros veiktie pētījumi. Ar to rezultātiem iespējams iepazīties projekta interneta vietnē www.balticflows.eu.

Miniaturizācija padara iespējamus jaunus maza izmēra un mazu izmaksu tehnoloģiskos risinājumus. Tas nosaka pakāpenisku pāreju no individuālām, konkrētajam risinājumam piemērotām, iekārtām ar augstām izmaksām, uz mazām mazu izmaksu iekārtām, kuras var tikt uzstādītas masveidā. Nākotnē miniatūri mazu izmaksu ūdens analīžu risinājumi, kuri varēs pārraidīt datus reālā laika režīmā, tas radīs iespējas izveidot plašas teritorijas aptverošas un reālā laikā strādājošas ūdens uzraudzības sistēmas. Turklāt šīs iekārtas varētu pašas ražot savai darbībai nepieciešamo enerģiju no ūdens straumes enerģijas, līdz ar to iztiekot bez enerģijas piegādes infrastruktūras risinājumiem.

Pašreiz projekts Baltic Flows ir jau praktiski pabeigts. Tas tika uzsākts 2013. gada oktobrī un to ir plānots pabeigt 2016. gada septembrī. Par projektā iegūtajām zināšanām un izdarītajiem darbiem var uzzināt tā interneta vietnē www.balticflows.eu (angļu valodā).

Šis projekts ir saņēmis finansējumu no Eiropas Savienības 7. ietvarprogrammas koordinācijai, atbalstam un kapacitātes stiprināšanai saskaņā ar dotāciju līgumu nr. 319923.

15.08.2016.

The Latvian Journal of Physics and Technical Sciences **to subscribers**

Scientific institutes are offered to subscribe to

the Latvian Journal of Physics and Technical Sciences for 2017

The Latvian Journal of Physics and Technical Sciences publishes articles on the latest national and international breakthroughs in power engineering, smart grids, solid state physics and nanotechnology. The authors of articles are industry professionals, power engineers and physicists.

The electronic version of the journal is published by De Gruyter publishing house, which is one of the leading scientific publishers in the world.

The journal is included in the following international databases: ESCI, SCOPUS, EBSCO, VINITI.

The journal ranking indicators:
Source Normalized Impact per Paper (SNIP): 2015: 0.332,
SCImago Journal Rank (SJR): 2015: 0.174
Impact per Publication (IPP) 2015: 0.200

The journal website: http://www.fei-web.lv